AD-A103 734 COLD REGIONS RESEARCH AND ENGINEERING LAB HANOVER NH F/G 8/12
REVIEW OF THERMAL PROPERTIES OF SNOW, ICE AND SEA ICE,(U)
JUN 81 Y YEN
UNCLASSIFIED CRREL-81-10 NL

END
DATE FILMED
10-81
DTIC

# CRREL
## REPORT 81-10

LEVEL II

# *Review of thermal properties of snow, ice and sea ice*

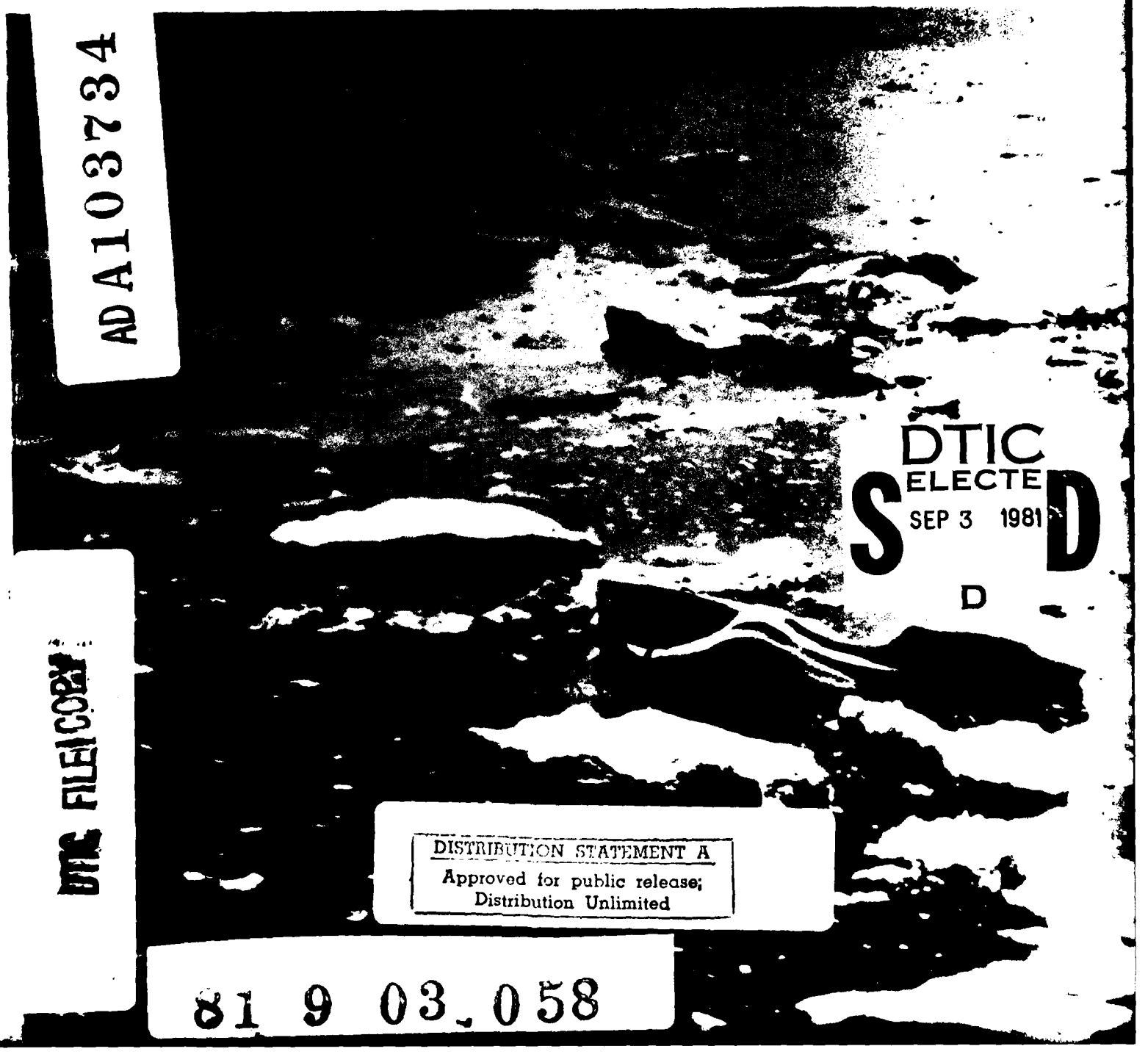

AD A103734

DTIC ELECTE SEP 3 1981 S D

DTIC FILE COPY

DISTRIBUTION STATEMENT A
Approved for public release;
Distribution Unlimited

81 9 03.058

# CRREL Report 81-10

# *Review of thermal properties of snow, ice and sea ice*

Yin-Chao Yen

June 1981


| Accession For | |
|---|---|
| NTIS GRA&I | X |
| DTIC TAB | ☐ |
| Unannounced | ☐ |
| Justification | |
| By | |
| Distribution/ | |
| Availability Codes | |
| Dist | Avail and/or Special |
| A | |

DTIC
ELECTE
1981
D


UNITED STATES ARMY CORPS OF ENGINEERS
COLD REGIONS RESEARCH AND ENGINEERING LABORATORY
HANOVER, NEW HAMPSHIRE, U.S.A.

Approved for public release; distribution unlimited.

Unclassified

SECURITY CLASSIFICATION OF THIS PAGE *(When Data Entered)*

| REPORT DOCUMENTATION PAGE | READ INSTRUCTIONS BEFORE COMPLETING FORM |
|---|---|
| 1. REPORT NUMBER<br>CRREL Report 81-10 | 2. GOVT ACCESSION NO.<br>AD-A103734 | 3. RECIPIENT'S CATALOG NUMBER |
| 4. TITLE *(and Subtitle)*<br>REVIEW OF THERMAL PROPERTIES OF SNOW, ICE AND SEA ICE | 5. TYPE OF REPORT & PERIOD COVERED<br>6. PERFORMING ORG. REPORT NUMBER |
| 7. AUTHOR*(s)*<br>Yin-Chao Yen | 8. CONTRACT OR GRANT NUMBER*(s)* |
| 9. PERFORMING ORGANIZATION NAME AND ADDRESS<br>U.S. Army Cold Regions Research and Engineering Laboratory<br>Hanover, New Hampshire 03755 | 10. PROGRAM ELEMENT, PROJECT, TASK AREA & WORK UNIT NUMBERS<br>DA Project 4A151101A91D |
| 11. CONTROLLING OFFICE NAME AND ADDRESS<br>U.S. Army Cold Regions Research and Engineering Laboratory<br>Hanover, New Hampshire 03755 | 12. REPORT DATE<br>June 1981<br>13. NUMBER OF PAGES<br>34 |
| 14. MONITORING AGENCY NAME & ADDRESS*(if different from Controlling Office)* | 15. SECURITY CLASS. *(of this report)*<br>Unclassified<br>15a. DECLASSIFICATION/DOWNGRADING SCHEDULE |

16. DISTRIBUTION STATEMENT *(of this Report)*

Approved for public release; distribution unlimited.

17. DISTRIBUTION STATEMENT *(of the abstract entered in Block 20, if different from Report)*

18. SUPPLEMENTARY NOTES

19. KEY WORDS *(Continue on reverse side if necessary and identify by block number)*

Ice
Sea ice
Snow
Thermal properties

20. ABSTRACT *(Continue on reverse side if necessary and identify by block number)*

This treatise thoroughly reviews the subjects of density, thermal expansion and compressibility of ice; snow density change attributed to destructive, constructive and melt metamorphism; and the physics of regelation and the effects on penetration rate of both the thermal properties of the wire and stress level. Heat capacity, latent heat of fusion and thermal conductivity of ice and snow over a wide range of temperatures were analyzed with regression techniques. In the case of snow, the effect of density was also evaluated. The contribution of vapor diffusion to heat transfer through snow under both natural and forced convective conditions was assessed. Expressions representing specific and latent heat of sea ice in terms of sea ice salinity and temperature were given. Theoretical models were given that can predict the thermal conductivities of fresh bubbly ice and sea ice in terms of salinity, temperature and fractional air content.

DD FORM 1 JAN 73 1473 EDITION OF 1 NOV 65 IS OBSOLETE

Unclassified

SECURITY CLASSIFICATION OF THIS PAGE *(When Data Entered)*

## PREFACE

This report was prepared by Dr. Yin-Chao Yen, Chief, Physical Sciences Branch, Research Division, U.S. Army Cold Regions Research and Engineering Laboratory. The study was funded under the *In-House Laboratory Independent Research Program*, DA Project 4A161101A91D. The critical and constructive reviews of this manuscript by Dr. Kazuhiko Itagaki and Dr. Samuel Colbeck are greatly appreciated.

## CONTENTS



## ILLUSTRATIONS

Figure

## TABLES

## NOMENCLATURE

| | |
|---|---|
| $A$ | dimensional constant; activation energy |
| $a$ | wire radius; dimensional constant |
| $B$ | dimensional constant |
| $b$ | dimensional constant |
| $C$ | vapor concentration |
| $c_p, c$ | heat capacity |
| $C_1$ | fractional increase in snow density per meter water equivalent of load per hour at $\rho_s = 0$ and $\theta = 0°C$ |
| $C_2$ | dimensional constant of compaction parameter of snow ($m^3/mg$) |
| $C_3$ | dimensional constant (fractional settling rate at 0°C) |
| $C_4$ | dimensional constant |
| $D$ | diffusion coefficient |
| $F$ | load on the object |
| $\bar{F}$ | force per unit length |
| $G$ | air mass flow rate |
| $H$ | enthalpy |
| $h$ | thickness of a liquid layer |
| $L$ | latent heat |
| $M$ | molecular weight; molecular weight of air |
| $m$ | net sublimation per unit volume; mass; mass flux |
| $P$ | hydrostatic pressure; vapor pressure |
| $\Delta P_0$ | maximum excess pressure |
| $p$ | pressure; precipitate |
| $R$ | gas law constant |
| $s$ | fractional salt content; entropy per unit mass |
| $t$ | time |
| $T$ | temperature in kelvins |
| $U$ | internal energy |
| $V$ | volume of an object, ice; fractional volume content |
| $v$ | penetration velocity; volume per unit mass |
| $W_s$ | weight of snow above a given layer expressed in terms of water equivalent in meters |
| $w$ | mass of unfrozen water |
| $\alpha$ | thermal diffusivity; proportional constant |
| $\beta_T$ | ratio of vapor concentration to temperature |
| $\gamma$ | coefficient of thermal expansion |
| $\delta$ | thickness of coating; water layer |
| $\eta$ | viscosity coefficient of snow |
| $\eta_c$ | viscosity coefficient of snow when snow density is extrapolated to zero |
| $\theta$ | temperature in degrees Celsius |
| $\lambda$ | thermal conductivity |
| $\pi$ | 3.1416; total pressure |
| $\rho$ | density; thermal resistivity |
| $\sigma$ | salinity (grams of salt per gram of sea ice) |
| $\tau$ | time increment |
| $\phi$ | correlation coefficient |
| $\omega$ | compressibility |

### Subscripts

| | |
|---|---|
| a | air; adiabatic |
| b | brine |
| bi | bubbly ice |
| c | cubic |
| e | effective; experimental |
| f | fusion |
| h | precipitated hydrate |
| i | ice |
| ia | ice containing air bubbles |
| ℓ | liquid; linear; linear thermal boundary |
| m | melting; material; mean |
| n | nth layer |
| o | through air |
| p | pressure |
| s | snow; solid; sinusoidal boundary; sublimation; saturation; and distance increment |
| sa | snow containing air |
| se | snow (effective) |
| si | sea ice |
| t | isothermal, theoretical |
| v | volume; vapor |
| w | water |

# REVIEW OF THERMAL PROPERTIES OF SNOW, ICE AND SEA ICE

Yin-Chao Yen

## INTRODUCTION

This review was undertaken in an attempt to summarize and analyze as completely as possible the reported data on the various thermal properties of snow, ice and sea ice and to provide readily available information for practical use in the field of snow and ice research.

In the second section, research on the density, linear and cubic expansion coefficients and compressibility of ice is summarized. Slight variations in density due to various defects such as contamination (by solids as well as by air), aging, and crystallographic form are discussed. In the temperature range of practical interest in cold regions, both the linear and cubic coefficients of expansion can be satisfactorily expressed as linear functions of temperature. The reported work on isothermal and adiabatic compressibility is limited and the variation of results of different investigators is pronounced.

In the third section, snow density changes due to various metamorphism processes are discussed. These phenomena are important because of their effect on the physical and mechanical properties of snow and on the physical processes occurring within a snow mass.

The process of regelation is described in the fourth section. A great number of theoretical analyses and experimental works are thoroughly reviewed and compared. Discrepancies between the proposed theories and the experimental results are great. The relationships between the penetration velocity of the object passing through ice and the wire material, wire size, stress level and ice purity are also discussed. Knowledge of the physics of regelation may provide an insight into the processes of sintering and the development of intergranular bonds in snow.

In the fifth section, the heat capacity and thermal conductivity of snow and fresh-water ice over a great range of temperatures are reviewed, and expressions developed by regression analysis are presented. These properties control the rate of propagation of thermal waves through the snow and ice mass and indicate both the relative potential as a heat storage medium and the rate of heat dissipation. The effects of water vapor diffusion (under either natural or forced convection) on the temperature profile and mass redistribution within a snow layer are discussed, providing a basis for interpreting the field data.

Finally, a general discussion of the thermal properties of sea ice is given. Since sea ice is a much more complicated material to deal with than pure ice, and its composition (the relative proportion of its constituents) is strongly temperature- and time-dependent, few experimental studies have been reported. It is believed that predicted thermal properties of sea ice, based on some simplified sea ice structural models, give a good approximation of the real value. In this review, expressions relating specific heat, heat of fusion, density, thermal conductivity and air bubble content for some specific temperature ranges are given. Thermal conductivity models and methods of determining thermal diffusivity are also briefly described.

## DENSITY, THERMAL EXPANSION AND COMPRESSIBILITY OF ICE

### Density

According to a review work by Dorsey (1940), the bulk density of ice at 0°C and atmospheric pressure varies from 0.916 to 0.918 Mg/m$^3$. Barnes (1901) and Dantl and Gregora (1968) indicated that ice density $\rho_i$ decreases slightly with age. Nichols (1899) reported densities at 0°C of 0.91795, 0.91632 and 0.91603 Mg/m$^3$ for freshly formed natural ice, one-year-old natural ice and artificial ice frozen at low temperatures, respectively. However, Barnes found much smaller variation in the ice samples taken from

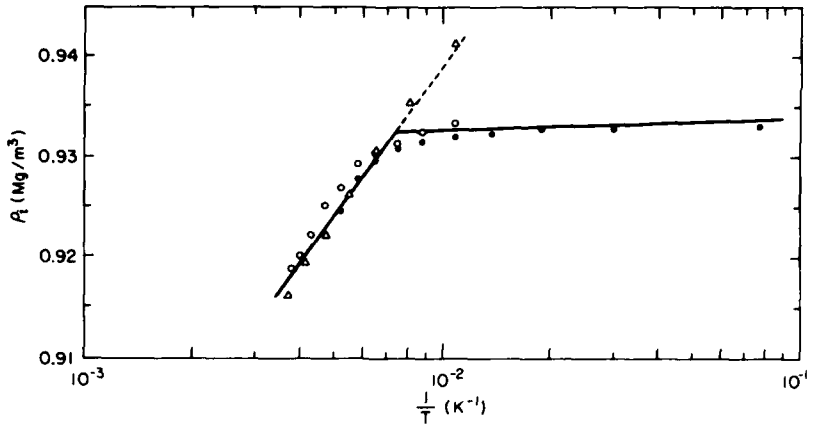


*Figure 1. Density of ice as a function of temperature. Δ—deduced by Lonsdale (1958) from the average of several diffraction measurements made prior to 1958. ○—deduced by Eisenberg and Kauzmann (1969) from X-ray diffraction measurements by LaPlaca and Post (1960). ●—deduced by Hobbs (1974) from X-ray diffraction measurements made by Brill and Tippe (1967).*

the St. Lawrence River; densities at 0°C of new, one-year-old and two-year-old ice were 0.91662, 0.91648 and 0.91637 Mg/m$^3$, respectively.

There are many other factors affecting the variation of the bulk density of ice $\rho_i$. These include the number and nature of the cracks, the degree of air entrainment, ice purity, dislocation, and stacking fault vacancy.

The true value of $\rho_i$, reported to be 0.9167 ± 0.00005 Mg/m$^3$, was determined by Ginnings and Corruccini (1947) using a Bunsen ice calorimeter; $\rho_i$ may also be deduced from measurements of the unit-cell parameters. Figure 1 shows $\rho_i$ versus $1/T$ from data obtained by Lonsdale (1958), Eisenberg and Kauzmann (1969) and Hobbs (1974). The value of $\rho_i$ at 0°C given by Lonsdale (0.9164 Mg/m$^3$) is in good agreement with that given by Ginnings and Corruccini. However, for lower temperatures, $\rho_i$ values given by LaPlaca and Post (1960) and Brill and Tippe (1967) are probably more reliable.

**Thermal expansion**

The coefficient of linear expansion $\gamma_\ell$ is a measure of the fractional change in length per unit change in temperature. Butkovich (1957) reported that the orientation of the *C*-axis, the type of ice (whether single or polycrystalline), and the grain size do not appreciably affect the values of the coefficient of linear expansion. Ice can be considered as an isotropic material with respect to thermal expansion in the temperature range 0° to -30°C. Figure 2 shows some of the most reliable measurements of $\gamma_\ell$ for bulk ice; it can be seen that $\gamma_\ell$ increases with increasing temperature. According to Jakob and Erk (1928) and Dantl (1962), $\gamma_\ell$ is negative at about 70 K and lower. Hamblin (Powell 1958) reported that $\gamma_\ell$ values measured in a direction parallel to the *C*-axis are about 1.8% and 10% greater than those in a direction perpendicular to the *C*-axis at 273.1 and 73.1K, respectively.

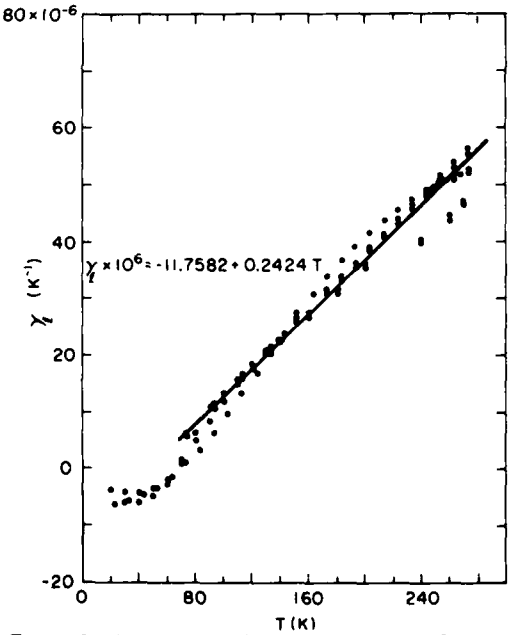


*Figure 2. Coefficient of linear expansion of ice at atmospheric pressure. Points represent the data of Jakob and Erk (1928), Powell (1958), Butkovich (1959) and Dantl (1962). Samples consisted of polycrystals, single crystals and single crystals parallel and perpendicular to the C-axis. (The data of Dantl are taken from his graph and therefore may introduce a slight error.)*

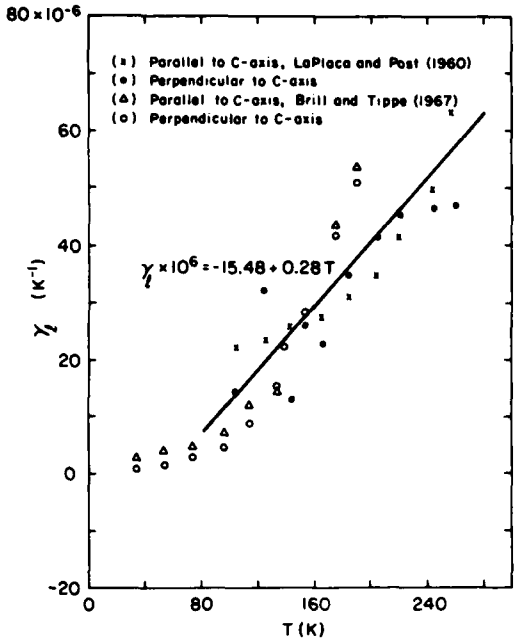


*Figure 3. Coefficient of linear expansion of ice deduced from measurements of the temperature dependence of the unit-cell parameters.*

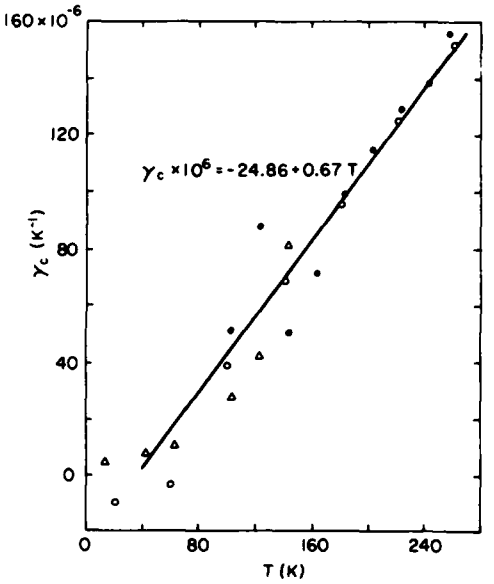


*Figure 4. Coefficient of cubic expansion of ice as a function of temperature at atmospheric pressure. ○—deduced by Leadbetter (1965) from linear expansion coefficients given by Powell (1958) and Dantl (1962). ●—deduced by Eisenberg and Kauzmann (1969) from measurements of the unit-cell parameters made by LaPlaca and Post (1960). Δ—deduced by Hobbs (1974) from measurements of the unit-cell parameters made by Brill and Tippe (1967).*

Dantl found that $D_2O$ ice has a slightly higher value for $\gamma_\ell$ throughout the temperature range studied. His $\gamma_\ell$ values at 240, 260 and 270 K are believed to be in error. For temperatures $T$ greater than 80 K, the data can be represented by

$$\gamma_\ell \times 10^6 = -11.7582 + 0.2424\,T \qquad (1)$$

with a relatively higher correlation coefficient $\phi$ of 0.9736. Therefore, for engineering applications, it is quite adequate to compute $\gamma_\ell$ from this expression, which is applicable in the temperature range from 80 to 273.1 K.

In Figure 2 the data points of Powell were calculated from two expressions:

$$\gamma_\ell \times 10^6 = 56.5 + 0.250\,\theta \qquad (2)$$

for measurements in a direction parallel to the $C$-axis and

$$\gamma_\ell \times 10^6 = 55.5 + 0.248\,\theta \qquad (3)$$

for measurements in a direction perpendicular to the $C$-axis, where $\theta$ is temperature in degrees Celsius.

Values for $\gamma_\ell$ can also be deduced from measurements of the temperature dependence of the unit-cell parameters of ice. Values obtained this way may be more significant that those obtained by direct diatometric measurements because they depend only on changes in the dimensions of the lattice and not on the texture of the ice. However, X-ray measurements may involve larger errors than bulk measurements at low temperatures. Figure 3 shows $\gamma_\ell$ values deduced from the temperature dependence of the unit-cell parameters from more recent measurements made by LaPlaca and Post (1960) and Brill and Tippe (1967). The magnitude and general trend seem to be in fair agreement with the measurements for bulk ice shown in Figure 2. For temperatures from 80 to 273 K, $\gamma_\ell$ can be fairly represented by $\gamma_\ell \times 10^6 = -15.48 + 0.28\,T$. There seems to be no consistent difference between $\gamma_\ell$ values parallel and perpendicular to the $C$-axis in either set of measurements. The irregular pattern of the data by LaPlaca and Post must be due to a lack of sample purity or to experimental conditions. For practical purposes, eq 1 can be used to calculate $\gamma_\ell$ values for temperatures ranging from 80 to 273 K.

Figure 4 shows the coefficient of volumetric expansion $\gamma_c$ of ice as a function of temperature at atmospheric pressure. The data were taken from Hobbs (1974) [omitting two $\gamma_c$ values at mean temperatures of 163.1 and 183.1 K from measurements of the unit-cell parameters made by Brill and Tippe (1967)]. A linear regression analysis results in an expression of

$\gamma_c \times 10^6 = -24.86 + 0.67\,T$ with a fairly high correlation coefficient of 0.94. Though there are some discrepancies among the three sets of data, the general trend of $\gamma_c$ variation with temperature is evident: It increases with temperature and it becomes negative when $t$ is lower than about 50 K.

### Compressibility

The compressibility of a substance is defined as the change in its volume per unit change in hydrostatic pressure. If the change takes place at constant temperature, it is called isothermal compressibility $\omega_t$. If the change takes place without energy exchange with the surroundings, it is called the adiabatic compressibility $\omega_a$.

As usual, the limited data available did not agree. Bridgman (1912) reported an $\omega_t$ of $37 \times 10^{-6}$ /bar at 273.1 K and one atmosphere; this value is about three times higher than the value $12 \times 10^{-6}$ at 70°C and 300 atmospheres reported by Richard and Speyers (1914). Bridgman later revised his values as shown in Figure 5, which indicates the effect of $T$ on $\omega_t$. With the exception of $\omega_t$ at 273 K, the five points given by him lie close to a line on a semi-log plot. The values for $\omega_t$ can be given by $\omega_t \times 10^6 = 14.20 \exp(0.0018\,T)$.

Values for $\omega_a$ obtained by Leadbetter (1965) based on the elastic constant measurements of ice by Bass et al. (1957) and Zarembovitch and Kahane (1964) are also shown in Figure 5 and can be expressed as $\omega_a \times 10^6 = 10.55 \exp(0.0007\,T)$. Leadbetter indicated that the uncertainty in $\omega_a$ values for temperatures below -30°C is probably less than 10%. For temperatures above -30°C, $\omega_a$ values are accurate to about 5%. Dantl (1969) also presented $\omega_a$ values based on measurements of the elastic constant and provided the following expression:

$$\omega_a \times 10^6 = 11.94\,(1 + 1.653 \times 10^{-3}\,\theta + 3.12 \times 10^{-6}\,\theta^2) \qquad (4)$$

where $\omega_a$ is in $bar^{-1}$ and $\theta$ is in degrees Celsius. A few points from this expression are also shown in the figure. Note that Dantl's $\omega_a$ values are much lower than Leadbetter's values and that they decrease sharply as temperatures decrease. According to Dantl's data, $\omega_a$ becomes negative around 120 K. On the other hand, Leadbetter found that the variation of $\omega_a$ with $T$ was very slight. This discrepancy must be due to a variety of factors, for example, the conditions of the experiment and the origin, age and purity of the sample.

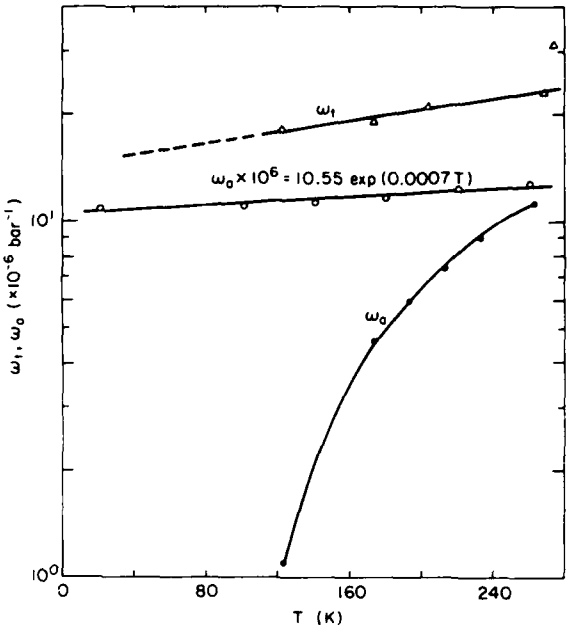


*Figure 5. Isothermal and adiabatic compressibility of ice. Δ—data of Bridgman (Richard and Speyers 1914). ○—deduced by Leadbetter (1965) from elastic constants measured by Bass et al. (1957) and Zarembovitch and Kahane (1964). ●—data from Dantl (1969).*

## DENSITY CHANGES IN SNOW

### Compaction

The compaction of snow layers can be seen graphically in seasonal snow layer depth profiles obtained during several investigations (Bader et al. 1939). Kojima (1967) and Yosida (1963) presented quantitative expressions for density change due to compaction. Based on many observations of the change in depth of various layers (with no change in water equivalent), the following relation between snow density and overburden weight of snow was established:

$$\frac{1}{\rho_s}\frac{\partial \rho_s}{\partial t} = \frac{W_s}{\eta} \qquad (5)$$

where $\rho_s$ is the snow density ($Mg/m^3$), $t$ is the time (hr), $W_s$ is the weight of the snow above the layer for which the density change is being computed and is expressed in water equivalent (m), and $\eta$ is the viscosity coefficient of snow (m·hr) and is a constant for a given density, temperature, and snow type. Kojima indicated that $\eta$ and $\rho_s$ can be expressed by

$$\eta = \eta_c \exp(C_2 \rho_s) \qquad (6)$$

where $\eta_c$ is the value of $\eta$ when $\rho_s = 0$, and $C_2$ is a constant to be determined. If eq 5 and 6 are combined and $C_1 = \eta_c^{-1}$, eq 5 becomes

$$\frac{1}{\rho_s}\frac{\partial \rho_s}{\partial t} = C_1 W_s \exp(-C_2 \rho_s). \tag{7}$$

Kojima reported $C_1$ values of 2.6–9.0/m·hr and $C_2$ values of 21 $m^3$/Mg. Equation 7 accurately described the data of Kojima except for the cases of low-density snow layers, wind-packed snow, and depth-hoar layers. For low-density and wind-packed layered snow, the density due to compaction increased at a higher rate than that predicted using the $C_1$ and $C_2$ values obtained for ordinary snow. However, for depth-hoar layered snow, the density increase was at a much lower rate.

Based on his observations and work in polar regions, Mellor (1964) claimed that the value of $C_1$ varied with snow temperature and type. He provided the following relation of $\eta_\theta$ (at $\theta$°C) to $\eta_0$ (at 0°C):

$$\frac{\eta_\theta}{\eta_0} = \exp\left[-\frac{A}{R}\frac{T_0 - T}{T \cdot T_0}\right] \tag{8}$$

where $T$ and $T_0$ are the absolute temperatures in K that correspond to $\theta$° and 0°C, respectively. $A$ is the activation energy ($\sim 10^4$ cal/mol) and $R$ is the universal gas constant ($\sim 2$ cal/mol K). For temperatures normally experienced in areas with seasonal snow cover, the value of $A/(RTT_0)$ can be taken as 0.08/K (if $T_0 = 273$ K and $T = 253$ K). Thus, to include the effect of temperature on the density change due to compaction, eq 7 can be rewritten as

$$\frac{1}{\rho_s}\frac{\partial \rho_s}{\partial t} = C_1 W_s \exp(-C_2 \rho_s) \exp[-0.08(T_0 - T)] \tag{9}$$

where $C_1$ is now the fractional increase in density ($m^{-1}$ $hr^{-1}$) at 0°C and $\rho_s = 0$.

**Destructive metamorphism**

Under equilibrium temperature conditions, water molecules move on the snow crystals by the processes of sublimation and condensation in order to decrease the surface free energy. Freshly fallen snow crystals have a very high ratio of surface area to mass. The water molecule migration process (called destructive metamorphism) changes these sharp-edged crystals into aggregates of smooth grains that are rounded, oblong or irregular. As a result, the snow settles and increases in density. These phenomena have been observed and photographed by Bader et al. (1939) and Yosida (1955) and were found to be temperature-dependent. Yosida reported that the rate of increase in grain diameter at -20°C is about 60% of that at -6°C. The effect of settling on density change was found to be important only in the early stages after snowfall. Gunn (1965) indicated that layers of new snow settled at about 1% per hour immediately after snowfall; he found this rate to be independent over the density range from 0.05 to 0.15 Mg/$m^3$. Destructive metamorphism was found to be a slow process where $\rho_s$ was higher than 0.25 Mg/$m^3$.

There is no established mathematical expression describing density changes due to destructive metamorphism. Anderson (1976), using the same reasoning as that given in relating the density increase due to compaction, hypothesized the following relation:

$$\frac{1}{\rho_s}\frac{\partial \rho_s}{\partial t} = C_3 \exp[-C_4(T_0 - T)] \tag{10}$$

for $\rho_s < \rho_d$ and

$$\frac{1}{\rho_s}\frac{\partial \rho_s}{\partial t} = C_3 \exp[-C_4(T_0 - T)] \exp[-46(\rho_s - \rho_d)] \tag{11}$$

for $\rho_s > \rho_d$. $C_3$ is the fractional settling rate ($hr^{-1}$) at 0°C for $\rho_s < \rho_d$, $C_4$ is a settling parameter ($K^{-1}$), $\rho_d$ is the density below which the settling rate for snow equals $C_3$, and 46 is an empirical dimensional constant ($m^3$/Mg) necessary to lower the settling by a factor of 100 when $\rho_s - \rho_d = 0.1$ Mg/$m^3$ [that is, $\exp(-46 \times 0.1) = \exp(-4.6) \simeq 1/100$].

**Constructive metamorphism**

Constructive metamorphism is the process of vapor transfer within the snow cover due to the temperature gradient. Vapor is removed from one crystal by sublimation and deposited on another by condensation. The change in density with respect to time is

$$\frac{\partial \rho_s}{\partial t} = m + \frac{\partial C}{\partial t} \tag{12}$$

where $m$ is the net sublimation (the net amount of vapor that undergoes a phase change) and $\partial C/\partial t$ is the rate of change of saturated vapor concentration in the void space of snow. When the effective diffusion coefficient of water vapor $D_e$ varies with snow depth, the net sublimation can be expressed as

$$m = D_e \frac{\partial^2 C}{\partial z^2} + \frac{\partial D_e}{\partial z}\frac{\partial C}{\partial z} - \frac{\partial C}{\partial t} \tag{13}$$

where $z$ is one of the coordinates in the direction of diffusion.

For water-vapor-saturated porous media such as snow, the value of vapor concentration $C$ is solely a function of temperature; that is, $C = f(T)$ disregarding the surface energy effect. Substituting eq 13 into eq 12 yields

$$\frac{\partial \rho_s}{\partial t} = D_e f' \frac{\partial^2 T}{\partial z^2} + f' \frac{\partial D_e}{\partial z} \frac{\partial T}{\partial z} + D_e f'' \left(\frac{\partial T}{\partial z}\right)^2 \tag{14}$$

where $f'$ and $f''$ are the first and second partial derivatives of vapor concentration with respect to temperature ($\partial C/\partial T$ and $\partial^2 C/\partial T^2$). If $D_e$ is assumed to be solely a function of temperature for a given depth [that is, $\partial D_e/\partial z$ can be replaced by $(\partial D_e/\partial T)(\partial T/\partial z)$], eq 14 becomes

$$\frac{\partial \rho_s}{\partial t} = D_e f' \frac{\partial^2 T}{\partial z^2} + \left(f' \frac{\partial D_e}{\partial T} + D_e f''\right)\left(\frac{\partial T}{\partial z}\right)^2. \tag{15}$$

For a prolonged thermal gradient near the bottom of the snow cover, constructive metamorphism leads to the formation of depth hoar. Kojima (1967) reported that well-established depth-hoar layers compact at a greatly reduced rate. DeQuervain (1973) also indicated that layers in a state of advanced constructive metamorphism usually do not settle unless there is structural collapse.

**Melt metamorphism**

Melt metamorphism is the change in snow structure due to melt-freeze cycles and the change in crystals due to the presence of liquid water. In general, melting decreases the depth of snow cover, and all or a portion of the melt-water may be retained and may refreeze, causing an increase in the ice content of the snow cover. A melt–refreeze cycle increases the density of the affected portion of the snow cover by several percent. Wakahama (1968) reported that the grain size increased at a faster rate as the amount of water increased, but the density (initial $\rho_s = 0.39$ Mg/m$^3$) did not change unless the snow was subjected to a load. Colbeck (1973) studied the problem theoretically and arrived at essentially the same conclusions about grain growth and density change. Both Wakahama and Colbeck indicated that when water saturation is high, the rate of compaction should increase. However, these conditions normally do not occur in a snow cover except over impermeable ice layers or at the ice/snow interface. Therefore, for high-density, wet snow with nearly spherical grains, the rate of increase in density should be similar to that for dry snow. For fresh, low-density snow, it seems reasonable to expect that the presence of liquid water will accelerate destructive metamorphism, thus increasing the settling rate.

## REGELATION

The change in equilibrium melting temperature $dT_m$ due to a small change in hydrostatic pressure $dp$ is expressed thermodynamically as

$$\frac{dT_m}{dp} = \frac{v_\ell - v_s}{s_\ell - s_s} \tag{16}$$

where $v$ and $s$ are volume and entropy, respectively, of a unit mass of material, and subscripts $\ell$ and $s$ refer to liquid and solid, respectively. Equation 16 can be rewritten as

$$dT_m = \frac{T_m(v_\ell - v_s)}{L_f} dp = -A\, dp \tag{17}$$

where $L_f$ is latent heat of fusion and is defined as $T_m(s_\ell - s_s)$. For ice, $v_s > v_\ell$; therefore, $T_m$ decreases with increasing hydrostatic pressure.

The first theoretical value of $A = 0.00745$°C/bar was calculated by Thomson (1849), and Thomson's brother (1850) verified experimentally that $T_m$ is lowered by pressure. The modern accepted experimental value of $A$ (0.00738°C/bar) was obtained by Moser (1929). However, for a high pressure form of ice, $v_\ell > v_s$; consequently, $T_m$ increases with increasing pressure. It should also be noted that under hydrostatic tension, ice should be able to exist at temperatures well above 0°C, but this has never been verified experimentally.

The melting point is also changed by non-hydrostatic stress. The phase equilibrium of a solid under non-hydrostatic stress was examined theoretically by Gibbs (1877). He reported that the stress component to be used to determine $dT_m$ is the stress normal to the interface. On the other hand, Verhoogen (1951) indicated that the relevant stress is the mean stress in the solid. Kamb (1961) analyzed these two theories as well as the most recent ones and concluded that only that of Gibbs has any validity.

The lowering of $T_m$ of ice by pressure has been used to explain the phenomenon of regelation, a term which was introduced by Tyndall and Huxley (1857) to account for Faraday's observation that two pieces of ice adhere when they are brought into contact. However, regelation has been used more specifically

to describe the passage of a weighted object through a block of ice, the compaction of wet snow (Colbeck 1979), and the movement of glaciers over obstacles on their bed (Weertman 1957). Bottomley (1872) conducted the first experiments on the passage of a wire through ice and explained his observations in terms of Thomson's pressure-melting theory. The pressure of the wire causes the ice underneath it to melt and form a thin layer of water, which moves around the upper side of the wire, where it freezes. As the ice continues to melt and refreeze, the wire passes through it. Bottomley concluded that the wire has to be a sufficiently good thermal conductor to permit the latent heat of fusion needed to melt the ice to be conducted through the wire from its upper side, where the water is refreezing and liberating heat. Turpin and Warrington (1884) repeated Bottomley's experiment using wires of different thermal conductivities. They reported that the speed of a wire passing through the ice increased with the wire conductivity, but they failed to develop a simple relation between the two parameters. Kojima (1954) conducted a number of experiments on regelation using six wires with differences in either thermal conductivity or wire diameter.* He concluded, as had Bottomley (1872) and Turpin and Warrington (1884), that the most important factor for regelation is the thermal conductivity of the wire material and that the contribution due to heat conducted along the wire from the surrounding air was insignificant. He also indicated that the viscoelastic property of ice did not play a role in the process.

Recently a series of theoretical and experimental papers have been published on this subject. This includes the work of Telford and Turner (1963), Nye (1967, 1973), Frank (1967), Townsend and Vickery (1967), Nunn and Rowell (1967), Hahne and Grigull (1969, 1972), and Drake and Shreve (1973). Nye (1967) analyzed the problem theoretically, taking into account the flow of heat and water. He showed that if the thermal resistance of the object was the dominant factor, then the wire speed depends on the volume of the object and not its shape. He further reported that for a sphere or a cylindrical wire, the thickness of the water film is always uniform and does not depend on the speed.

Nye developed the following equation:

$$v = FA\,\lambda/L_f v\rho_i \qquad (18)$$

where $v$ is the steady state velocity, $F$ is the load on the object, $L_f$ is the latent heat of fusion, $\rho_i$ is the ice density, $\lambda$ is the thermal conductivity of the object of volume $V$, and $A$ is a constant defined in eq 17. Figure 6 summarizes the results of Nye's calculations. Metal wires used in laboratory experiments usually fall into regions 1A or 2A; poor conductors are usually in 1B or 1C. The water film was found to be very thin; for example, for a steel wire 1 mm in diameter, the theory predicts a water film thickness of 0.36 $\mu$m.

To test Nye's theoretical treatment, Townsend and Vickery (1967) conducted experiments with spheres and discs that were about 10 mm in diameter and made of different materials. Their results for spheres are shown in Figure 6. The observed velocities were up to three times lower than those predicted by eq 18. However, for discs, the velocities varied from nearly equal to the predicted value to 33 times slower. Nunn and Rowell (1967), using cylindrical specimens, showed similar discrepancies for metallic wires (by a factor of up to 18) but found reasonable agreement with the theory when testing insulated wires.

Frank (1967) speculated on the effect of water-film stability on the rate of penetration of the object. For high-thermal-conductivity objects, the freezing surface at the rear of the object is likely to be unstable, causing the water to separate from it in an extended wake and resulting in slower penetration than the theory predicts. For objects with low thermal conductivity, there would be instability in the forward melting surface. However, Frank believed it would not produce any significant deviations from Nye's theory.

These studies were all conducted when the ice was nearly at its melting point. The only significant study relating the effect of ice temperature on the speed of wire passage is reported by Telford and Turner (1963). In their experiment, a steel wire 0.45 mm in diameter was hung across a block of ice. The results are shown in Figure 7. The velocity increased by a factor of 10 as the temperature increased from -3.5° to -0.7°C. As the temperature increased to -0.5°C, the velocity increased discontinuously by a factor of 200. This steep jump was attributed to the onset of pressure melting, since the load on the wire lowered the melting point by about 0.5°C. The much lower velocities at temperatures well below -0.5°C could not have been due to pressure melting. Telford and Turner attempted to deduce the wire motion mechanism at lower temperatures by considering the flow of a thin Newtonian shear layer of viscous fluid around the wire. By assuming that the fluid acts as a liquid-like layer (Fletcher 1962, 1968), the velocity $v$ may be shown to be related to the thickness $h$ and viscosity $\eta$ of this layer by

* In one case a combination of high- and low-conductivity wires was used. This was done by fastening linen cords on both ends of a copper wire of 10-cm length and laying it over the ice pillar so that the copper wire part was on its top.

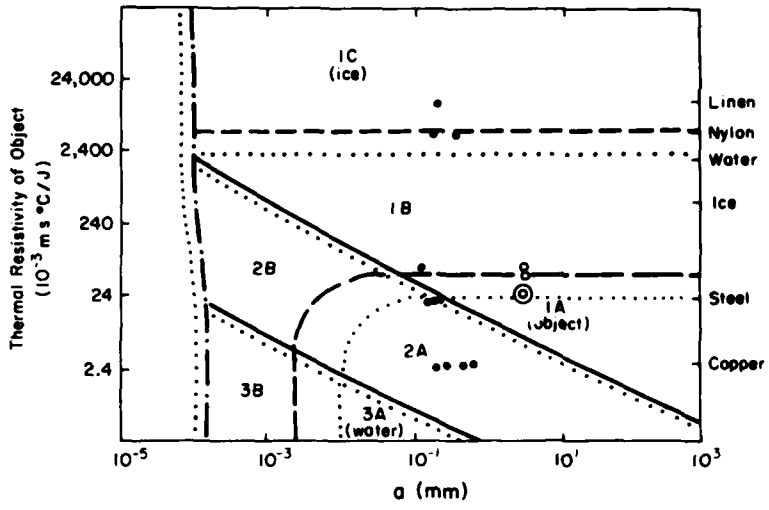


*Figure 6. Theoretical and experimental data on the passage of an object through ice by regelation. (Adapted from Nye 1967.) In case 1, $T_r \ll 1$; in case 2, $T_r \simeq 1$; and in case 3, $T_r \gg 1$, where $T_r$ is the ratio of the temperature drop across the water to that across the object. In subdivision A the heat flows mainly through the object and the water, in B the heat is divided between this path and that through the ice, and in C the heat flows mainly through the ice. The controlling thermal resistance (ice, object or water) is noted in parentheses. Dotted boundaries refer to spherical objects; all others refer to cylindrical objects. ○ – Townsend and Vickery's experiments on spheres. ● – Nunn and Rowell's experiments on wires.*

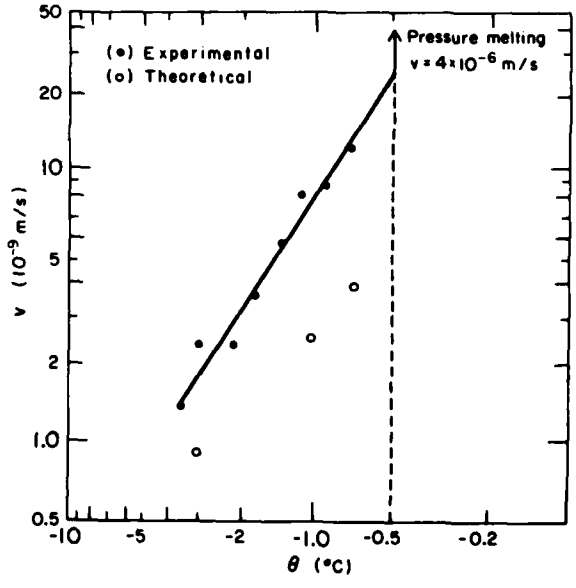


*Figure 7. Velocity of a steel wire moving through ice as a function of temperature. (Adapted from Telford and Turner 1963.) The wire diameter was 0.45 mm, the load was 2.1 kg, and the thickness of ice was 10 mm. At the temperature marked by the arrow, the velocity changed discontinuously by a factor of 200 due to pressure melting. The theoretical values are based on Fletcher's liquid-like layer theory.*

$$v = \frac{\bar{F}}{2\pi\eta}\left(\frac{h}{a}\right)^3 \qquad (19)$$

where $\bar{F}$ is the force per unit of wire length and $a$ is the wire radius. The variation of velocity with temperature might therefore be explained by a change in layer thickness with temperature, as predicted by Fletcher (1962). The computed values of $v$ (from eq 19), with the thickness and temperature relationship given by Fletcher and the value of $\eta$ appropriate to supercooled water, are also shown in Figure 7; they compare fairly well with the experimental data.

Equation 19 predicts a linear relation between $v$ and $\bar{F}$, but the experimental results showed that $v$ is proportional to $\bar{F}_3$, which is similar to the finding by Glen (1952) for the creep of polycrystalline ice. However, there are great differences between the values of activation energy in Glen's results and those shown in the figure. Therefore, the wire motion is not due to a simple creep phenomenon.

Hahne and Grigull (1972) considered the regelation of ice as a heat conduction problem. In developing their model, they reasoned that while the wire is moving through the ice, the layer immediately below the wire melts. The water containing the heat of fusion is pressed around the wire to the upper side, where it refreezes and releases the heat of fusion, which is then conducted to the melting zone. For wires of thermal conductivity greater than that of ice, say copper, most of the heat is conducted through the wire. For materials such as Perlon, however, the heat is predominantly conducted through the ice around the wire. The wire surface temperature should be lowest on the leading side and highest on the trailing side. Hahne and Grigull solved the heat conduction equation using simplified boundary conditions for the linear case (when the heat flows through the wire) and the sinusoidal case (when heat flows around the wire). The penetration rate was found to be

$$v = \frac{T(\nu_i - \nu_w)}{4\rho_i L_f^2}\,\Delta P_0 \left[\frac{1}{(a/\lambda_m)+(\delta/\lambda_w)+(\Sigma\delta_n/\lambda_n)} + \frac{1}{a/\lambda_i}\right] \qquad (20)$$

for the linear thermal boundary and

$$v = \frac{T(\nu_i - \nu_w)}{\pi\rho_i L_f^2}\,\Delta P_0 \left[\frac{1}{(a/\lambda_m)+(\delta/\lambda_w)+(\Sigma\delta_n/\lambda_n)} + \frac{1}{a/\lambda_i}\right] \qquad (21)$$

for the sinusoidal case, where $\nu_i$ and $\nu_w$ are the specific volumes of ice and water, respectively, $\Delta P_0$ is the maximum excess pressure, $\delta$ is the water layer thickness, $\delta_n$ is the thickness of the $n$th coating, and $\lambda$, $\lambda_w$, $\lambda_i$ and $\lambda_n$ are the thermal conductivity of the wire material, the water, the ice and the $n$th coating, respectively.

To calculate the penetration rate, the value of $\delta$ is needed. By considering the problem as one of one-dimensional creeping flow, values of $\delta$ can be approximated by trial and error from

$$\frac{6\mu a\pi}{\delta_\ell^2}\left(\frac{a\pi}{\delta_\ell}\frac{\rho_i}{\rho_w} - 1\right) = \frac{4\rho_i L_f^2}{T(\nu_i - \nu_w)} \left[1/\left[\frac{1}{(a/\lambda_m)+(\delta_\ell/\lambda_w)+(\Sigma\delta_n/\lambda_n)} + \frac{1}{a/\lambda_i}\right]\right] \qquad (22)$$

for the linear case and

$$\frac{6\mu a}{\delta_s^2}\left(\frac{a\pi}{\delta_s}\frac{\rho_i}{\rho_w} - 1\right) = \frac{\rho_i L_f^2}{T(\nu_i - \nu_w)} \left[1/\left[\frac{1}{(a/\lambda_m)+(\delta_s/\lambda_w)+(\Sigma\delta_n/\lambda_n)} + \frac{1}{a/\lambda_m}\right]\right] \qquad (23)$$

for the sinusoidal case.

Hahne and Grigull used bare copper and Perlon wires in their study because the wires differed greatly in thermal conductivity. The results can be represented by a log-log plot of $v$ versus $a$ (Fig. 8). For copper wire, the dependence of $v$ on $a$ is nearly identical for all the three pressure values used [$v \propto (a)^{-0.5}$]. This is also true for Perlon wire, except that the dependence of $v$ on $a$ is stronger [$v \propto (a)^{-0.1}$]. Cross plots of $v$ versus pressure $p$ for any specific value of $a$ used in the study revealed the pressure dependence of $v \propto (p)^{1.333}$ for both copper and Perlon wires (Fig. 9). Consequently the penetration rate can be represented by

$$v = 1.674\,(p)^{1.333}\,(a)^{-0.50} \qquad (24)$$

for copper and

$$v = 0.114\,(p)^{1.333}\,(a)^{-1.0} \qquad (25)$$

for Perlon wires.

The effect of thermal conductivity $\lambda_m$ on $v$ was evaluated for a wire radius of 0.25 mm and pressures of 5, 7.5 and 10 bars by estimating values of $v$ for Perlon wire from eq 25. It can be expressed as

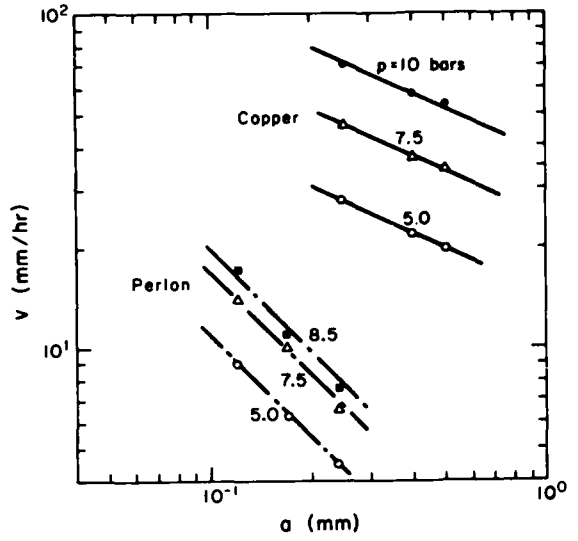


*Figure 8. Penetration velocity as a function of wire radius and material under various pressures. (From data obtained by Hahne and Grigull 1972.)*

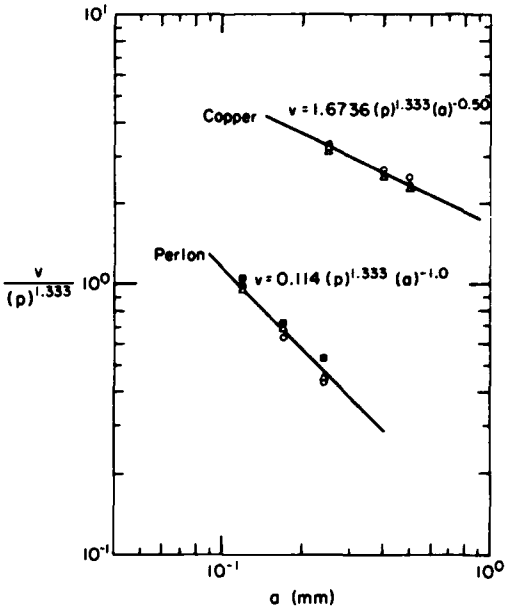


*Figure 9. Penetration velocity as functions of pressure and wire radius for two materials that differ in thermal conductivities.*

$$v = 0.0624(p)^{1.333}\,(\lambda_m)^{0.284}. \qquad (26)$$

The general relationships among $v$, $p$, $a$ and $\lambda_m$ can not be established due to the lack of data. However, the data available show that when $a > 0.25$ mm, the dependence of $v$ on $\lambda_m$ is greater; when $a < 0.25$ mm, the influence of $\lambda_m$ on $v$ is reduced.

The assumption and verification of the existence of a very thin film of water on the surface of ice and in any gap between ice and any other material (Fletcher 1962, Nakamura 1966) led Weyl (1951) to hypothesize that different penetration speeds for different materials should be explained on the basis of film thickness rather than thermal conductivity. To examine Weyl's reasoning, Hahne and Grigull (1972) compared the speed of silver-plated copper and iron wires with that of silver wire. If the surface material and the ice would dominate the regelation phenomenon, the velocities of bare silver and silver-plated copper wires should be the same for corresponding diameters and pressures. They found, however, that the same difference in velocity of bare copper and iron wires is maintained for the corresponding silver-plated wires, indicating that the dominant factor in wire movement through ice is thermal conductivity. When varnish-coated copper and iron wires are tested, the value of $v$ and the difference in $v$ between them are drastically reduced, indicating the significant effect of wire thermal conductivity on penetration rate. When Perlon wire (which has a thermal conductivity of the same order of magnitude as the varnish-coated copper and iron wires) is tested, $v$ is also of the same order of magnitude. From these studies, it is clearly demonstrated that the conductivity of the wire material and not the formation of a thin water layer between the wire and ice affects the wire speed.

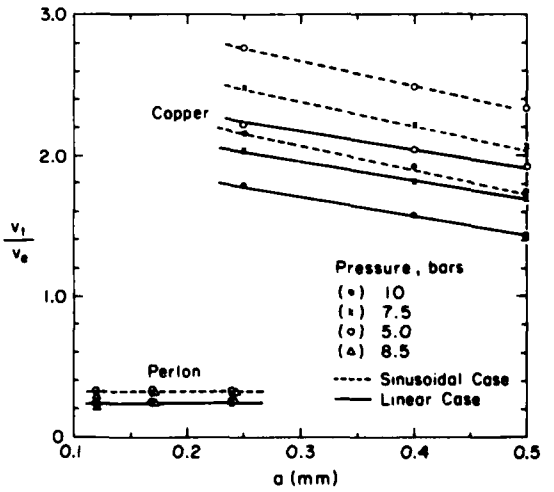


*Figure 10. Ratio of theoretical to experimental penetration velocities of Hahne and Grigull (1972) as functions of pressure, wire radius and material.*

**Table 1. Comparison of theoretical and experimental results on penetration velocity $v$.**

| | | | | Nye/Nunn and Rowell | | | Nye/Hahne and Grigull | | | |
|---|---|---|---|---|---|---|---|---|---|---|
| Material | $\lambda$ (W/m K) | $a$ ($10^{-3}$ m) | $P$ (bar) | $v_{tn}$ (mm/hr) | $v_{enr}$ (mm/hr) | $v_{tn}/v_{enr}$ | $v_{t\ell}$ (mm/hr) | $v_{ts}$ (mm/hr) | $v_{tn}/v_{ts}$ | $v_{ts}/v_{enr}$ |
| Silver | 419 | 0.25 | 3.48 | 120.24 | 7.20 | 17 | 46.60 | 56.41 | 2.13 | 6.47 |
| Copper | 385 | 0.36 | 2.41 | 63.72 | 3.60 | 18 | 24.53 | 30.00 | 2.12 | 6.81 |
| | | 0.55 | 3.83 | 74.88 | 6.12 | 12 | 29.24 | 35.94 | 2.08 | 4.78 |
| | | 0.79 | 5.42 | 83.52 | 7.20 | 12 | 31.81 | 39.06 | 2.64 | 4.42 |
| | | 0.79 | 1.81 | 27.79 | 2.52 | 11 | 10.62 | 13.04 | 2.13 | 4.21 |
| Carbon- | 50 | 0.19 | 8.42 | 110.88 | 9.00 | 12 | 44.48 | 55.99 | 1.98 | 4.94 |
| Steel/Iron | | 0.23 | 3.62 | 39.96 | 4.68 | 8.6 | 16.05 | 20.24 | 1.97 | 3.42 |
| | | 0.23 | 7.24 | 79.92 | 9.72 | 8.2 | 32.10 | 40.48 | 1.97 | 3.30 |
| | | 0.28 | 5.96 | 54.72 | 5.76 | 9.5 | 22.05 | 27.84 | 1.96 | 3.82 |
| | | 0.28 | 2.98 | 27.40 | 2.88 | 9.5 | 11.02 | 13.92 | 1.96 | 3.82 |
| Nylon/Perlon | 0.25 | 0.21 | 7.65 | 5.04 | 5.04 | 1.0 | 2.04 | 2.60 | 1.94 | 0.41 |
| | | 0.43 | 3.72 | 1.20 | 1.73 | 0.69 | 0.48 | 0.62 | 1.94 | 0.28 |
| | | 0.43 | 5.58 | 1.80 | 2.59 | 0.69 | 0.73 | 0.93 | 1.94 | 0.28 |

$v_{tn}$ = theoretical velocity by Nye (1967).

$v_{enr}$ = experimental velocity by Nunn and Rowell (1967).

$v_{t\ell}$ = theoretical velocity by Hahne and Grigull (1972) with linear boundary.

$v_{ts}$ = theoretical velocity by Hahne and Grigull (1972) with sinusoidal boundary.

Figure 10 shows the comparison between experimental results with bare wires and Hahne and Grigull's theoretical results based on the simplified heat conduction model. For copper wire, the ratio $v_t/v_e$ (where $v_t$ and $v_e$ are the theoretical and experimental penetration velocities, respectively) reaches a value of about 2.70 at 5.0 bars and $a$ = 0.25 mm with sinusoidal boundary conditions. This ratio increases as pressure decreases. However, it decreases as the wire radius increases for both the linear and sinusoidal cases. For Perlon wires, the ratio for the sinusoidal case is about 33% of the experimental value, and the effect of pressure can be considered to be insignificant.

Table 1 shows some comparisons of the theoretical results of Nye (1967) and Hahne and Grigull (1972) and the experimental work of Nunn and Rowell (1967). As indicated by the ratio $v_{tn}/v_{ts}$, the results of Hahne and Grigull using a sinusoidal thermal boundary ($v_{ts}$) are about half of those predicted by Nye ($v_{tn}$) for both metallic and insulated wires with great differences in thermal conductivity. Furthermore, the ratio of $v_{t\ell}$ (the penetration rate based on a linear thermal boundary) to $v_{enr}$ (the experimental results of Nunn and Rowell) is about 2.5 times lower than the ratio $v_{tn}/v_{enr}$ for metallic wires. (This ratio is not shown in the table.) Because of the different parameters used in Hahne and Grigull's experiment, a direct comparison with Nunn and Rowell's work can not be made. However, the results of Hahne and Grigull were consistently much higher. Since contamination, either on the wire surface or in the ice, decreases the wire speed, higher speeds are considered to be more reliable. The great discrepancies shown by $v_{tn}/v_{enr}$ can be attributed to too high values of $v_{tn}$ and too low values of $v_{enr}$.

The most recent and most comprehensive theoretical and experimental work on pressure melting and regelation of ice is that of Drake and Shreve (1973). They controlled temperature more precisely, used much smaller driving stresses, and watched the process and its after-effects more closely than did other investigators. The wires were made of copper, chromel and nylon (polyamide) with diameters ranging from 0.12 to 0.50 mm and $\lambda_m$'s ranging from 0.245 to 388 W/m K. They reported that the wire speed increases nonlinearly at all but the lowest driving stresses; at a stress of about 1 bar it jumps sharply but continuously and reversibly by an amount ranging from six-fold for nylon wires to 60-fold for copper wires (Fig. 11). Above this transition the speeds of copper wires are as low as one-eighth of those predicted by Nye, although the speeds of nylon and chromel are about the same as predicted. Below the transition the speeds of all wires are much less than predicted.

All wire speeds are significantly reduced by air bubbles in the ice. Drake and Shreve noticed that the wires leave a trace below the transition that consists of widely scattered, generally tiny bubbles of unfrozen water; above the transition the trace grades from numerous bubbles of water and vapor for highly conductive wires to a central flat layer of water for poorly conductive ones.

Measurements of the fractional volume of water in the trace show that above the transition, heat flows to

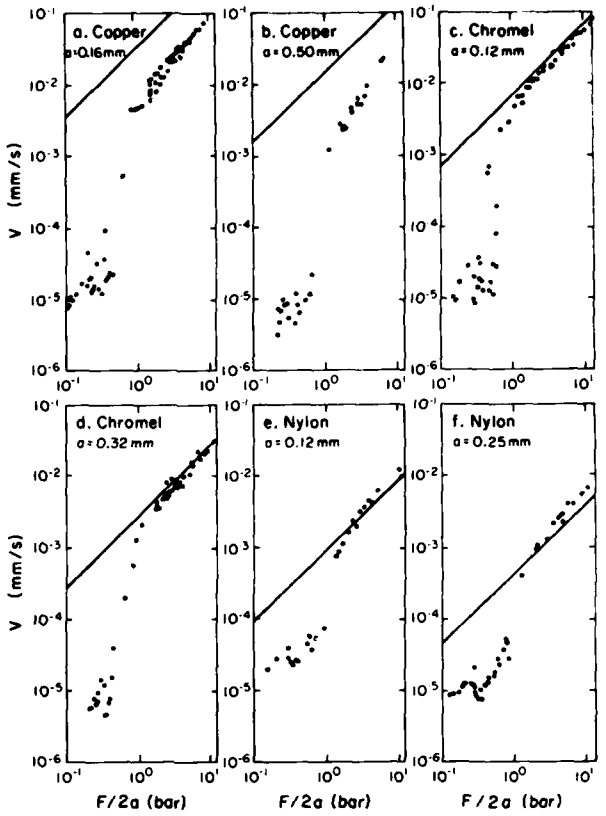


*Figure 11. Penetration velocities as functions of wire material, wire radius and stress level. Dots represent the data of Drake and Shreve (1973). The solid lines represent the theoretical work of Nye (1967).*

the moving wire from the surrounding ice. The non-linearity and low speed below the transition are due to the accumulation of solutes in the water layer around the wire; they concentrate toward the rear, lowering the freezing temperature and reducing the heat flow toward the melting front. The transition occurs when the temperature at the rear reaches the triple point corresponding to the existing local pressure. With increasing driving stress, the mean pressure around the wire increases and the mean temperature decreases, causing heat to flow toward the wire and causing formation of the trace, which carries away the solutes. For highly conductive wires the trace is bubbly because of the Frank instability (1967) of the freezing surface, which permits fingers of water and vapor to grow until pinched off by surface tension. For poorly conductive wires the non-linearity above the transition is mainly due to the additional melting at the front of the wire and the change in pressure distribution around the wire associated with the formation of the trace. For highly conductive wires the non-linearity and the unexpected slowness above the transition are mainly due to the supercooling required for a finite rate of freezing, which, like the presence of dissolved solutes, lowers the freezing temperature at the rear of the wire.

The work of Tozuka et al. (1979) is the most recent addition to the literature on this subject. In their experiment, copper and nylon wires of various radii were used and experiments using both commercial ice and ice doped with hydrogen fluoride were conducted in a room maintained at 1°C; the pressure ranged from 2 to 15 bars. They observed a sharp jump in copper wire speed (about 1.5 times) at pressures around 5 bars. [This is in sharp contrast to the 60-fold jump in wire speed at pressures around 1 bar reported by Drake and Shreve (1973).] In the case of nylon wires, however, the transition pressure has never been observed. (Drake and Shreve observed a 6-fold increase in speed for Perlon wires.)

The findings of Tozuka et al. concerning the effect of wire radius on speed were essentially consistent with the data obtained by Hahne and Grigull (1972). For low thermal conductivity wires (nylon and Perlon), the

wire speeds were found to be inversely proportional to the wire radius ($1/a$); for copper wires, the speeds were proportional to $(1/a)^{0.3}$ [versus $(1/a)^{0.5}$ derived from Hahne and Grigull's data].

Tozuka et al. also studied the effect of thermal conductivity on wire speed. At pressures below the transition point (such as 2.4 bars), measured speeds per unit pressure ($v/p$) were much smaller than those expected from the theory (Nye 1967) and had a larger scatter regardless of thermal conductivity. For pressures greater than the transition (such as 8 bars), speeds of medium thermal conductivity wires such as chromel and constantan were about the same as predicted from the theory. But in the case of copper wire, with its much higher thermal conductivity value, the theoretical wire speed was three times larger than the measured one. On the other hand, the measured speed for nylon wires, which are poor conductors, was greater than the theoretical one by about 40%.

The effects of impurity on wire speed were also reported by Tozuka et al. They indicated that the abrupt change in wire speed at the transition was mainly caused by impurities in the ice. They demonstrated this by measuring the temperature difference between the top and bottom sides of the wire.

Regardless of the uncertainties, however, the experimental and theoretical results as a whole clearly demonstrate that the long-accepted explanation of the motion of wires through ice as a process of pressure melting and regelation is basically correct. The large qualitative and quantitative discrepancies between the simple theory and the experimental observations are largely due to the neglect of the dissolved solutes in the water layer around the wire, of the formation of a trace behind the wire, whose geometry is governed by the Frank instability, and of the supercooling required to freeze water at a finite rate.

## THERMAL PROPERTIES OF SNOW AND FRESH-WATER ICE

### Heat capacity of snow and ice

The heat capacity is defined as the heat required for a unit of mass to rise one unit of temperature at constant pressure $c_p$ or at constant volume $c_v$. Mathematically it is defined as

$$c_p = \left(\frac{\partial H}{\partial T}\right)_p \quad \text{or} \quad c_v = \left(\frac{\partial U}{\partial T}\right)_v \tag{27}$$

where $H$ and $U$ are enthalpy and internal energy per unit mass, respectively. Since the heat needed to warm up the air and vapor in the interstices is very small, the heat capacity of dry snow and ice are essentially equal. The value of $c_v$ can be computed from $c_p$ by

$$c_p - c_v = \frac{\gamma_c^2 VT}{\omega_T} \tag{28}$$

where $V$ is the volume of ice, $\gamma_c$ is the coefficient of volumetric expansion, and $\omega$ is the compressibility. The value of $c_v$ is about 3% less than $c_p$ at the melting point, and the difference $(c_p - c_v)$ decreases with decreasing temperature.

The values of the heat capacities of ice made in the early twentieth century were reviewed and summarized by Dickinson and Osborne (1915) and Dorsey (1940). Giauque and Stout (1936), in an extensive study, reported $c_p$ values of hexagonal ice over temperatures ranging from 15 to 273 K. Flubacher et al. (1960) obtained $c_p$ values for hexagonal ice in the range from 2 to 27 K. Sugisaki et al. (1968) also made extensive measurements of $c_p$ for amorphous, cubic and hexagonal ice between 20 and 250 K. Most recently, Ashworth (1972), using a new technique, determined values of $c_p$ between 50 and 270 K. Figure 12 shows all the experimental data on $c_p$ for hexagonal and cubic ice. The data were divided into three or four temperature ranges [i.e., 15-50 K, 50-95 K (or 15-95 K), 95-150 K and > 150 K] and subjected to linear regression analysis. For each range $c_p$ is expressed as $c_p = A + BT$. The constants $A$ and $B$ and the correlation coefficients $\phi$ are listed in Table 2.

The data from all the investigations are consistent, as the high values of $\phi$ indicate. The effect of axis-orientation is within the experimental error. The linear representation of the data can be used to determine the value of $c_p$ at any specific temperature. For example, $c_p$ at the normal melting point is 37.7 J/mol K, about one-half of the heat capacity of liquid water. The value of $c_p$ decreases with decreasing $T$ and, as expected, approaches zero at 0 K.

Anderson (1976) gives an expression for $c_i$ as

$$c_i = 1.6738 + 0.1327T \tag{29}$$

**Table 2. Constants $A$ and $B$ in $c_p = A + BT$ and $\phi$.**

| Temp. range (K) | $A$ | $B$ | $\phi$ |
|---|---|---|---|
| 15-50 | -2.2171 | 0.2094 | 0.9920 |
| 50-95 | -0.0035 | 0.1597 | 0.9892 |
| 15-95 | -0.8994 | 0.1710 | 0.9931 |
| 95-150 | 2.2841 | 0.1350 | 0.9817 |
| >150 | 2.7442 | 0.1282 | 0.9737 |

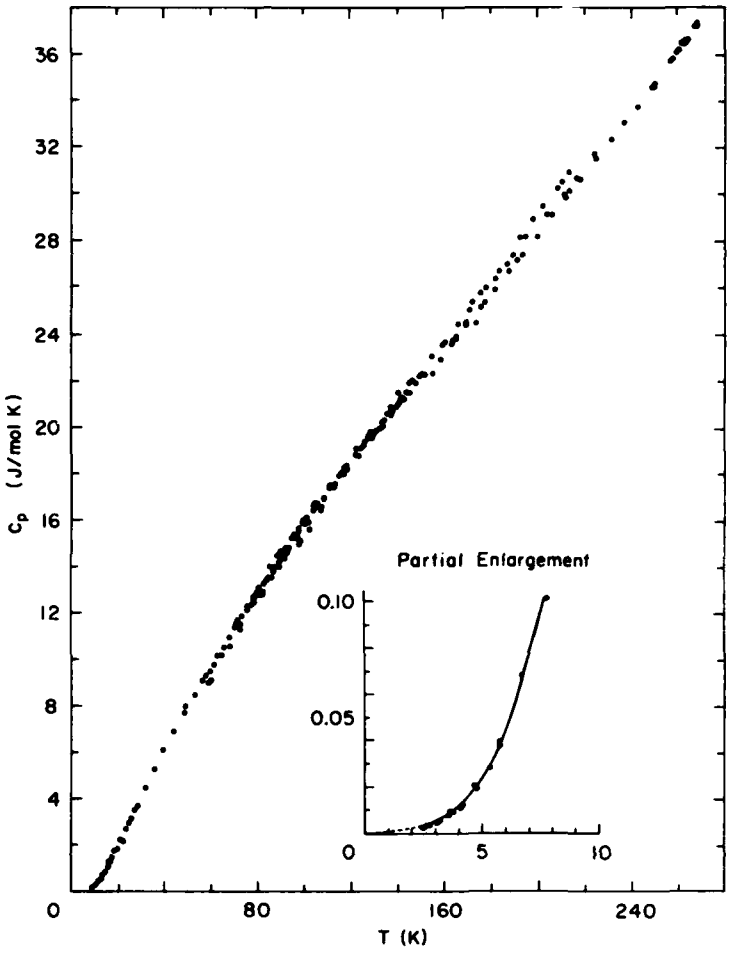


*Figure 12. Specific heat of ice. Points represent the data of Giauque and Stout (1936), Flubacher et al. (1960), Sugisaki et al. (1968) and Ashworth (1972). Samples consisted of cubic and hexagonal ice.*

where $c_i$ is the specific heat of ice. At 193 K, eq 29 shows $c_i$ to be 0.2 J/mol K less than the value computed from the highest temperature range in Table 2. At 273 K, however, it shows $c_i$ to be 0.055 J/mol K higher.

**Latent heat**

The change in enthalpy $dH$ associated with a change in phase of a material at constant pressure $p$ is given by

$$dH = dU + pdV \qquad (30)$$

where $dU$ and $dV$ are the changes in internal energy and volume per unit mass of material, respectively. The latent heat of fusion of ice $L_f$ is defined as the change in enthalpy when a unit mass of ice is converted isothermally and reversibly into liquid water. Because the term $pdV$ is rather small in comparison to other terms, $L_f$ is nearly equal to the change in internal energy. Measurements of $L_f$ made prior to 1925 have been reviewed by Smith (1925) and those up to 1940 by Dorsey (1940). Many early measurements are in error because the effect of impurities in ice was not taken into account properly. The most reliable value for $L_f$ at 0°C and standard atmospheric pressure is 33.5 kJ/kg, reported by Rossini et al. (1952). The value of $L_f$ decreases linearly with decreasing temperature down to about -10°C and then decreases at a lower rate as the temperature decreases further (Fig. 13).

The latent heat of sublimation of ice $L_s$ represents the enthalpy change when a unit mass of ice is transformed isothermally and reversibly into water vapor at standard atmospheric pressure and at the ice-liquid-vapor triple point (273.16 K). Rossini et al. reported a value of 2838 kJ/kg. It is interesting that $L_f$ represents only about 12% of $L_s$; therefore, only about 12%

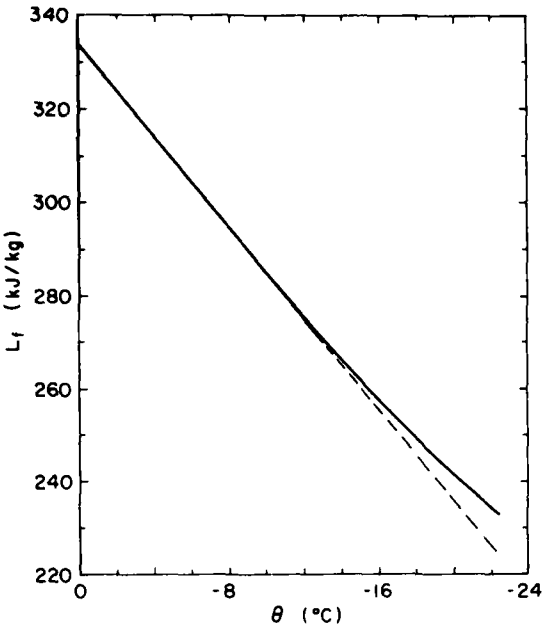


*Figure 13. Latent heat of ice as a function of temperature.*

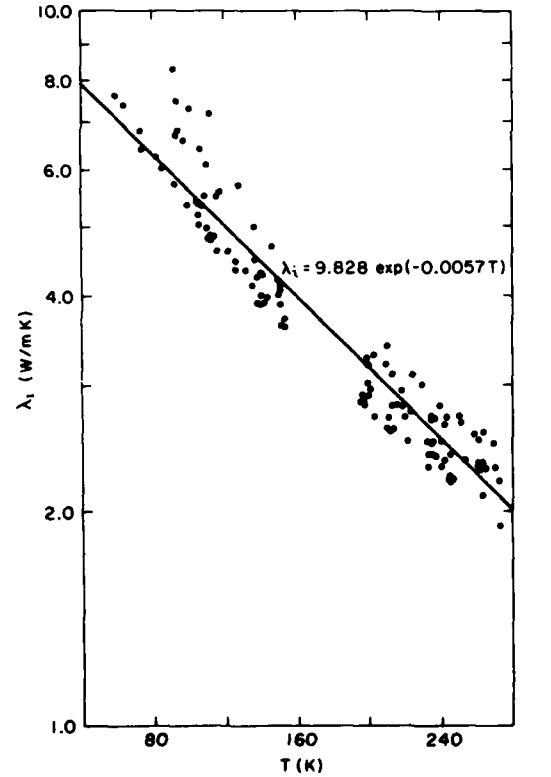


*Figure 14. Thermal conductivity of ice as a function of temperature. Points represent the data of Jakob and Erk (1929), Powell (1958), Ratcliffe (1962), Dean and Timmerhaus (1963), Wolfe and Thieme (1964), Dillard and Timmerhaus (1966) and Ashworth (1972).*

of the hydrogen bonds must break when ice melts. According to the data available, the value of $L_s$ remains practically constant (2838 kJ/kg) between 213.16 and 272.16 K.

**Thermal conductivity of ice**

Thermal conductivity $\lambda$ of a solid material is defined as the proportionality constant in the one-dimensional form of Fourier's law of heat conduction; that is,

$$q = -\lambda \frac{d\theta}{dz} \tag{31}$$

where $q$ is the heat flux in the direction normal to the temperature gradient $d\theta/dz$. Thermal conductivity usually depends on temperature $\theta$ and to a lesser extent on ice crystallographic orientation. Early work on thermal conductivity of ice $\lambda_i$ was reviewed by Powell (1958). At temperatures near 273 K, the value of $\lambda_i$ is about 2.2 W/m K, about four times as large as the $\lambda_w$ of water at 273 K. The increase in $\lambda_i$ with decreasing temperature reported by Lee (1905) was found to be much less rapid than that obtained by Jakob and Erk (1929). Landauer and Plumb (1956) reported no significant differences in the thermal conductivity coefficients of laboratory-grown single crystals, glacial single crystals and polycrystalline commercial ice, although the $\lambda_i$ along the C-axis of the single crystals appeared to be about 5% greater than that normal to the C-axis.

Figure 14 summarizes the recent measurements of $\lambda_i$ of polycrystalline ice by Ratcliffe (1962, taken from his best-fitted lines), Dillard and Timmerhaus (1966), Ashworth (1972), Dean and Timmerhaus (1963), and Wolfe and Thieme (1964). The relatively old data of Jakob and Erk (1929) and Powell (1958) are also shown. (For clarity of presentation, only one notation is used.) It seems as if each investigator provided data under a different set of techniques and conditions (such as sample purity, sample preparation, and methods for obtaining $\lambda$). Since there was a lack of data between 150 and 195 K, the data were divided at that gap. Regression analyses were made based on the expression

$$\lambda_i = a \exp(bT). \tag{32}$$

Table 3 shows the values of $a$, $b$ and $\phi$. The values for the whole temperature range had the highest correlation coefficient. Therefore, for practical purposes, it is suggested that one use

$$\lambda_i = 9.828 \exp(-0.0057\,T) \tag{33}$$

to compute the values of $\lambda_i$. The scattering of data is

**Table 3. Values of $a$, $b$ and $\phi$ from the regression analysis.**

| Temperature (K) | $a$ | $b$ | $\phi$ |
|---|---|---|---|
| <150 | 12.285 | -0.0076 | 0.7970 |
| >195 | 6.727 | -0.0041 | 0.5962 |
| all $T$ | 9.828 | -0.0057 | 0.9313 |

mostly due to differences in sample purity and preparation, adjustment of heat loss to the surroundings, and reproducibility of experimental data.

### Thermal conductivity of snow

The heat transfer processes in snow are much more complicated than in ice. In snow, heat is transferred by conduction through the interconnected ice grains, by conduction, convection and radiation across the air space, and by the movement of vapor by sublimation and condensation. In the determination of thermal conductivity, a temperature gradient is imposed, which subsequently establishes a vapor gradient and thus causes vapor diffusion. Therefore, the thermal conductivity of snow includes vapor diffusion. Thermal conductivity is expressed as effective thermal conductivity $\lambda_{se}$ (Yen 1962) to account for all the processes occurring in the snowpack. However, because of the low temperatures, the effect of radiation transfer is usually not significant.

Numerous investigators have reported the values of $\lambda_{se}$, and without exception, they empirically correlated their results with snow density (Fig. 15) as the sole parameter. The temperature ranges under which the data were obtained were usually not defined. The scattering of data is due to the snow conditions (such as aging and grain size distribution) and to the effects of vapor diffusion. Another factor may be the method used to determine $\lambda_{se}$. The transient method is more accurate than the steady-state technique, because in the transient method the heat loss to the surroundings during the experiment need not be assessed. Regardless of the difference in results from each investigator, all data can be reasonably represented by

$$\lambda_{se} = 2.22362\,(\rho_s)^{1.885} \qquad (34)$$

with a $\phi$ of 0.8614. It gives a reasonable value of $\lambda_i$ when extrapolated but a lower value of $\lambda_a$ when $\rho_s \to \rho_a$.

Pitman and Zuckerman (1967) appear to be the only investigators who systematically considered the effect of temperature on $\lambda_{se}$. They used vapor-grown ice crystals and conducted $\lambda_{se}$ measurements at -5°, -27°, and -88°C and at densities ranging from 0.1 to 0.6 Mg/m$^3$. A semi-log plot (Fig. 16) of their data (taken from their graph) shows three parallel straight lines (with the exception of $\rho_s$ = 0.1 Mg/m$^3$ at -88°C). Since the thermal conductivity of air at 0°C is about 0.024 W/m K, the straight line extrapolation to $\rho_s$ = 0.1 is probably a better representation of their data at -88°C. To determine the effect of temperature on $\lambda_{se}$ from these data, a plot of $\lambda_{se}$ (taken from Figure 16 at any specific $\rho_s$) versus $\theta$ was made and $\lambda_{se}$ was found to be proportional to $\theta$; that is, $\lambda_{se} \propto \exp(0.0088\theta)$. Finally, the data of Pitman and Zuckerman can be represented [except for the data for the lowest density ($\rho_s$ = 0.1)] by

$$\lambda_{se} = 0.0688 \exp(0.0088\theta + 4.6682\,\rho_s) \qquad (35)$$

as shown in Figure 17. Also shown in the figure are a few points taken from the work of Yen (1965) and Schwerdtfeger (1963a). For $\rho_s \to \rho_i$ = 0.917 and

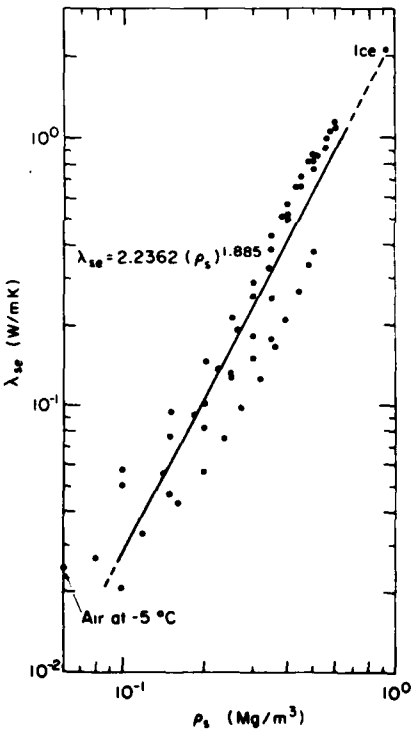


*Figure 15. Effective thermal conductivity of snow as a function of density. Points are derived from the equations of Abel's (1893), $\lambda_{se} = 2.8451(\rho_s)^2$; Jansson (1901), $\lambda_{se} = 0.0209 + 0.7950(\rho_s)^2 + 2.5104(\rho_s)^4$; Devaux (1933), $\lambda_{se} = 0.0293 + 2.9288(\rho_s)^2$; Kondrateva (1945), $\lambda_{se} = 3.5564(\rho_s)^2$; Bracht (1949), $\lambda_{se} = 2.0502(\rho_s)^2$; Sulakvelidze (1959), $\lambda_{se} = 0.5105\rho_s$; Yen (1962), $\lambda_{se} = 3.2217(\rho_s)^3$.*

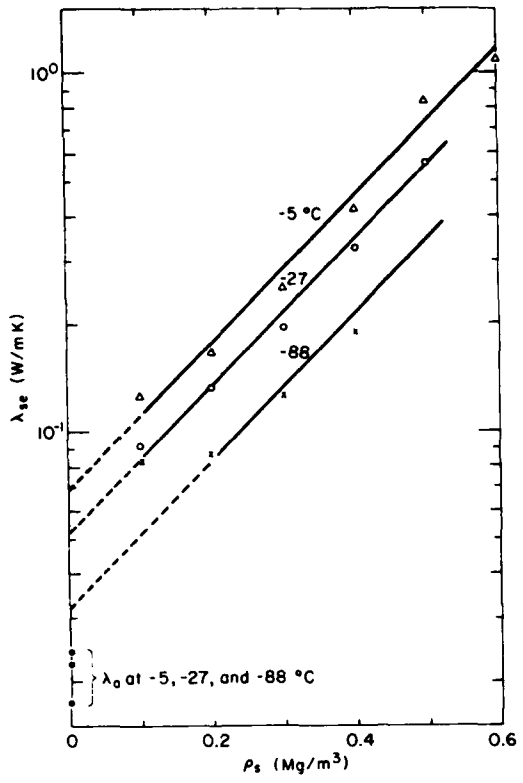


*Figure 16. Effective thermal conductivity of snow as functions of snow density and temperature.*

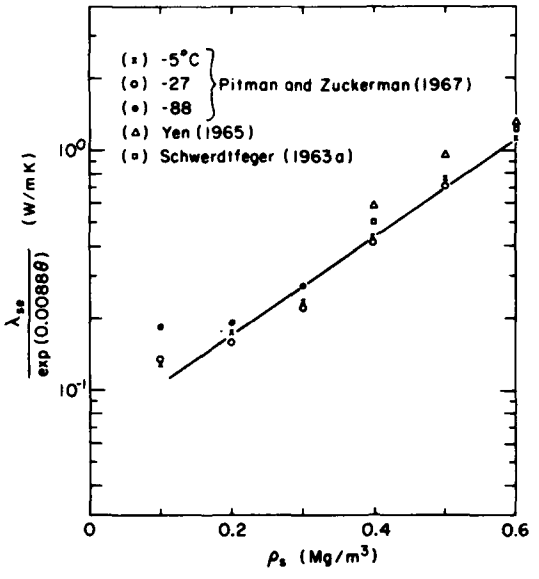


*Figure 17. Effect of temperature and snow density on effective thermal conductivity of snow.*

$\theta = 0°C$, the value of $\lambda_{se} \rightarrow \lambda_i = 4.98$ W/m K, which is about 2.3 times the accepted ice value of 2.2 W/m K at 0°C. For $\rho_s \rightarrow \rho_a$ and $\theta = 0°C$, $\lambda_{se} \rightarrow \lambda_a = 0.0688$ W/m K, which is about 2.8 times the value for air at 0°C ($\lambda_a = 0.0247$ W/m K).

Schwerdtfeger (1963a), using Maxwell's work on the electrical conductivity of heterogeneous media, derived theoretical expressions for $\lambda_{se}$. For dense snow, $\lambda_{se}$ is equivalent to $\lambda_{ia}$ and is given as

$$\lambda_{ia} = \frac{2\lambda_i + \lambda_a - 2\eta(\lambda_i - \lambda_a)}{2\lambda_i + \lambda_a - \eta(\lambda_i - \lambda_a)} \lambda_i \qquad (36)$$

where $\lambda_{ia}$ is the thermal conductivity of dense snow or ice containing air bubbles, and $\eta$ is the porosity and is related to $\rho_i$ and $\rho_s$ by $\eta = 1 - (\rho_i/\rho_s)$. Because $\lambda_a \ll \lambda_i$ and $\eta = 1 - (\rho_i/\rho_s)$, eq 36 becomes

$$\lambda_{ia} = \frac{2\rho_s}{3\rho_i - \rho_s} \lambda_i. \qquad (37)$$

For low density snow (down to 0.15 Mg/m$^3$)

$$\lambda_{sa} = \frac{(2+s)s}{(1+s)^2} \lambda_i \qquad (38)$$

where $s$ is a constant related to porosity by $\eta = 1/(1+s)^3$. When $\eta$ is given, the value of $s$ can be calculated. When $\rho_s = 0.4$ and $\eta = 0.536$, $s$ is found to be 0.212. From eq 38, $\lambda_{sa} = 0.7023$ W/m K for snow at 0°C. For very low density snow, a model is developed consisting of a suspension of small spherical particles in air not in contact with each other; the model is identical to eq 36 except for the interchange of $\lambda_i$ and $\lambda_a$, and the substitution of $\lambda_{sa}$ for $\lambda_{ia}$.

**Effective thermal diffusivity**

For a homogeneous, isotropic medium with constant physical properties, the effective thermal diffusivity $\alpha_e$ is the coefficient of the general heat conduction in Cartesian coordinates; that is,

$$\frac{\partial T}{\partial t} = \alpha_e \left( \frac{\partial^2 T}{\partial x^2} + \frac{\partial^2 T}{\partial y^2} + \frac{\partial^2 T}{\partial z^2} \right) \qquad (39)$$

where $\alpha_e$ is defined as $\lambda_e/\rho_s c_i$ and $\rho_s c_i$ is the volumetric specific heat of the medium.

Sulakvelidze (1959) formulated a heat transfer equation for porous media containing saturated vapor, water or ice at temperatures close to those of phase transition. This was done by including an evaporation-condensation

term in Fourier's heat conduction equation. For the case of one-dimensional heat transfer, the heat conduction equation becomes

$$\frac{\partial T}{\partial t} = \alpha_e \frac{\partial^2 T}{\partial z^2} + \frac{L_s}{c_i \rho_s} q \tag{40}$$

where $q$ is the intensity of sublimation of condensation ($Mg/m^3$) and can be expressed in terms of vapor concentration $C$ by

$$q = D_e \frac{\partial^2 C}{\partial z^2} - \frac{\partial C}{\partial t} \tag{41}$$

where $D_e$ is the effective water vapor diffusivity ($m^2/s$). Substitution of a prescribed function $f(T)$ for $C$ in eq 41 yields

$$q = D_e \frac{\partial^2 f}{\partial z^2} - \frac{\partial f}{\partial t}. \tag{42}$$

Equations 40 and 42 can be combined to give

$$\frac{\partial T}{\partial t} = \alpha_e \left[\frac{1 + D_e L_s/(\alpha_e c_i \rho_s) f'}{1 + (L_s/c_i \rho_s) f'}\right] \frac{\partial^2 T}{\partial z^2} + \frac{(L_s D_e / c_i \rho_s) f''}{1 + (L_s/c_i \rho_s) f'} \left(\frac{\partial T}{\partial z}\right)^2 \tag{43}$$

where $f'$ and $f''$ are first and second derivatives of $f$ with respect to $T$. Equation 43 describes the general processes of heat transfer taking place in a moist porous medium without including the effects of solar radiation or the changes in the amount of liquid water within the snow medium. Since the values of $c_i \rho_s$ are much greater than those of $L_s f'$, eq 43 can be reduced to

$$\frac{\partial T}{\partial t} = \left(\alpha_e + \frac{D_e L_s f'}{c_i \rho_s}\right) \frac{\partial^2 T}{\partial z^2} + \frac{L_s D_e f''}{c_i \rho_s} \left(\frac{\partial T}{\partial z}\right)^2. \tag{44}$$

When there is no vapor diffusion ($L_s = 0$), eq 4 reduces to the well-known Fourier equation

$$\frac{\partial T}{\partial t} = \alpha_e \frac{\partial^2 T}{\partial z^2}. \tag{45}$$

Once the function $f$ is chosen, the temperature distribution as a function of time can be computed.

**Heat transfer by water vapor diffusion in snow**

The diffusion coefficient $D$ for a binary system is a function of temperature, pressure and composition. For low pressure gas mixtures or dilute solutions, $D$ can be considered to be constant. In one-dimensional steady diffusion processes, Fick's law gives the mass flux $m$ as

$$m = -D \frac{dC}{dz} \tag{46}$$

where $dC/dz$ is the concentration gradient in the direction of diffusion.

Yosida (1950) was the first to study the effective diffusion coefficient $D_e$ for water vapor diffusing through snow. He reported $D_e$ values ranging from 0.7 to $1.0 \times 10^{-4}$ $m^2/s$, which is about four or five times larger than the diffusion coefficient $D_0$ for water vapor diffusing through air. When $\rho_s$ is in the range of 0.08 to 0.5 $Mg/m^3$, $D_e$ values remain more or less constant. By maintaining the lower boundary temperature higher than the upper one, he found that the effect of natural convection is insignificant. To explain the fact that $D_e > D_0$, Yosida pointed out that ice grains do not act as mere obstacles to the diffusion of water vapor as sand grains do; they produce water vapor themselves, thereby facilitating the mass transfer processes of sublimation and condensation. The heat transfer due to molecular vapor diffusion can be written in a form similar to Fourier's law of heat conduction:

$$q_v = -\beta_T D_e L_s \left(\frac{dT}{dz}\right) \tag{47}$$

where $q_v$ is the heat flux due to vapor diffusion and $\beta_T$ is the ratio of water vapor density to temperature. The product $\beta_T D_e L_s$ can be considered as $\lambda_v$, the thermal conductivity due to molecular diffusion. If $L_s$ = 2828.38 kJ/kg, $\beta_T = 0.39 \times 10^{-3}$ $kg/m^3$ K and $D_e = 0.85 \times 10^{-4}$ $m^2/s$, then $\lambda_v$ = 0.094 W/m K. Therefore, the molecular vapor diffusion plays a significant role in the process of heat transfer in low density snow.

**Heat and vapor transfer with forced convection**

The effects of air flow through snow on $\lambda_e$ and $D_e$ have been studied experimentally and theoretically and were reported in a series of papers by Yen (1962, 1963, 1965). For one-dimensional and steady-state cases, the governing equations for heat and vapor transfer can be summarized as follows. For heat transfer,

$$G c_a \frac{dT}{dz} + \frac{G M_w L_s}{M \pi} \frac{dP_s}{dz} + \lambda_e' \frac{d^2 T}{dz^2} = 0 \tag{48}$$

and for vapor transfer,

$$\frac{d^2 P_s}{dz^2} + \left(\beta - \frac{R_v T_m}{D_e' dP_s/dz} \frac{\partial \rho_s}{\partial t}\right) \frac{dP_s}{dz} = 0 \tag{49}$$

where $\rho_s$ is the saturation vapor pressure of snow, $c_a$ is the heat capacity of air, $R_v$ is the gas law constant for water vapor, $G$ is the air mass flow rate, $M_w$ and $M$ are the molecular weights of water and dry air, respectively, $\pi$ is the total pressure of the system, $T_m$ is the mean temperature of the system, $\lambda'_e$ and $D'_e$ are the effective thermal conductivity and diffusivity under forced convective flow, respectively, and $\beta$ is defined as $\beta = GR_vT_mM_w/M\pi D'_e$. To calculate $\lambda'_e$, only the steady-state temperature distribution is needed; to obtain $D'_e$, the density distribution before and after the experiment and the steady-state temperature distribution are required.

For unconsolidated snow with a density between 0.376 and 0.472 Mg/m$^3$, the value of $\lambda'_e$ can be expressed by $\lambda'_e = \lambda_e + 24.27G$ (Yen 1962), where $\lambda_e = 0.586$ W/m K and $G$ varies from $10\times10^{-3}$ to $40\times10^{-3}$ kg/m$^2$s. The value of 0.586 for $\lambda_e$ is consistent with the data reported by Kondrateva (1945). The value of $D'_e$ can be represented by $D'_e = 3.016\times10^{-3}\ (G+0.456\times10^{-3})^{1/2}$ when $G = 0$ and $D'_e \rightarrow D_e = 0.65\times10^{-4}$ m$^2$/s. As indicated in the previous section, Yosida (1950), using a completely different approach, reported a value of $0.85\times10^{-4}$ m$^2$/s for $D_e$. The differences may be partially due to the lower temperature in Yen's experiment.

For naturally compacted snow (Yen 1965), the following correlations for $\lambda'_e$ and $D'_e$ are valid for $\rho_s$ ranging from 0.50 to 0.59 Mg/m$^3$ and $G$ varying from $5\times10^{-3}$ to $32\times10^{-3}$ kg/m$^2$s.

$$\lambda'_e = 3.22(\rho_s)^2 + 25.1G \qquad (50)$$

and

$$D'_e = 0.65\times10^{-4} + 0.0513(\rho_s)^{3.20}(G)^{0.615} \qquad (51)$$

where $\lambda'_e$ and $D'_e$ are expressed in W/m K and m$^2$/s, respectively. When no air is flowing, $\lambda'_e$ reduces to $\lambda_e$, which is $3.22(\rho_s)^2$, and $D'_e$ becomes $D_e$, which is $0.65\times10^{-4}$ m$^2$/s. Both values are in agreement with experimental results (Yen 1962, 1963).

These results show that air flow has a considerable effect on the values of $\lambda'_e$ and $D'_e$ of both unconsolidated and naturally compacted snow. The increase in thermal conductivity and vapor diffusivity due to air flow is responsible for the small variations in snow density and temperature gradient near the surface layers of a snow cover.

## THERMAL PROPERTIES OF SEA ICE

Compared with fresh-water ice, whose physical properties are well known, sea ice is a relatively complex substance whose transformation to a completely solid mixture of pure ice and solid salts is attained only at low temperatures so extreme that they are rarely encountered in nature. The physical properties of sea ice thus depend strongly on salinity, temperature and age. Many of these properties are still not fully understood, particularly those important for the understanding of natural ice covers. In fact it appears to be safer to rely on theoretical values for thermal conductivity and specific heat, because precise measurement of these properties has always posed considerable difficulty. In the development of a suitable sea-ice model for calculating these quantities, an interesting progressive complexity appears: To calculate specific heat, knowledge of the composition alone is sufficient. Calculations of density also require consideration of air bubble content. Finally, to calculate the thermal conductivity, information on the spatial distribution of all components is necessary.

### Specific heat of sea ice

When sea water is cooled to its freezing point, pure ice crystals form. As freezing progresses, pockets of brine are cut off, so that the sea ice is composed of pure ice, brine, solid salt crystals and air bubbles (which have a negligible effect on the specific heat). The equilibrium salt concentration of the brine trapped in the ice depends on its temperature. When the sea ice temperature increases, the brine is diluted to a new equilibrium concentration by the melting of pure ice at the ice/brine interface. The specific heat of sea ice is the total of the heat required to raise the sea ice constituents (i.e. the pure ice and the brine) a unit of temperature and the heat associated with the phase change. The latter process leads to the fact that sea ice has an abnormally large specific heat.

Salinity is usually defined by oceanographers as the number of grams of dissolved solids in one kilogram of solution. This also applies to sea ice, and the mass of salt in grams per kilogram of sea ice is usually quoted in parts per thousand (‰). However, for convenience in deriving phase compositions of sea ice, the units "grams of salt per gram of sea ice" are often used. Based on the work of Malmgren (1927), it is believed that salinity is usually a good parameter in analyzing the thermal behavior of sea ice.

#### *Specific heat of ice between the freezing point and -8.2°C*

Within this temperature range, there is no significant substitution of ions in the ice lattice; thus, the brine in the interior cells has the same salt composition as the sea water from which the ice was formed. No precipitation of salt occurs in this temperature range (Fig. 18), and the specific heat depends essentially on the relative extent of the phase change and the specific heat of pure ice and the salt solution. The thermal

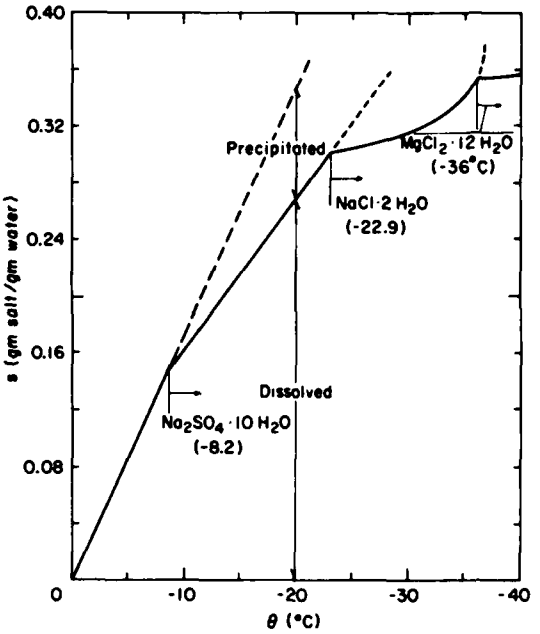


*Figure 18. Freezing point of brine as a function of fractional salt content. (After Schwerdtfeger 1963b.)*

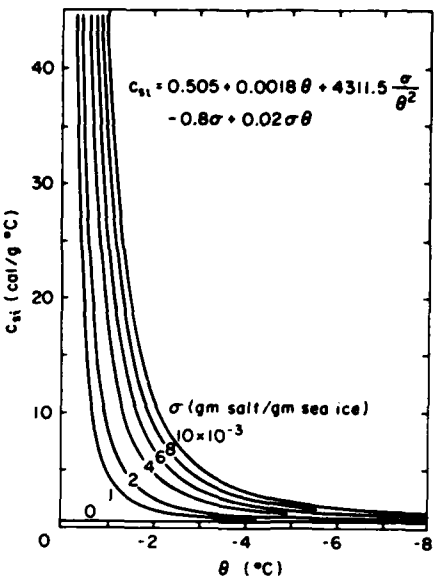


*Figure 19. Specific heat of sea ice as functions of temperature and salinity. (Modified from Ono 1966.)*

capacity of salt in $4^0/_{00}$ sea ice is on the order of 3.3472 J/kg K and can be considered to be negligible. The effects of heat of crystallization (or dilution) can also be neglected based on data quoted by Lange and Forker (1952). Consequently the specific heat of sea ice $c_{si}$ can be written as

$$c_{si} = -\alpha L_f \frac{\sigma}{s^2} + \frac{\sigma}{s}(c_w - c_i) + c_i \qquad (52)$$

where $\alpha$ is the coefficient of the relation between fractional salt content of the brine $s$ (in grams of salt per gram of water) and the temperature $\theta$, $\sigma$ is the salinity of sea ice (grams of salt per gram of sea ice), and $c_i$ and $c_w$ are the specific heat of pure ice and water, respectively. The relation between $s$ and $\theta$ is linear (Fig. 18), so $s = \alpha\theta$ ($\alpha$ is the slope of $s$ versus $\theta$, a negative quantity).

Replacing $s$ in eq 52, Pounder (1965) and Schwerdtfeger (1963b) both gave the expression

$$c_{si} = -\frac{\sigma}{\alpha\theta^2} L_f + \frac{\sigma}{\alpha\theta}(c_w - c_i) + c_i \qquad (53)$$

in which the term $\sigma c_i$ has been omitted for the case of natural sea ice. Ono (1966) used a somewhat different approach and developed the following expression:

$$c_{si} = 0.505 + 0.0018\theta + 4311.5\frac{\sigma}{\theta^2} - 0.8\sigma + 0.20\sigma\theta. \qquad (54)$$

The values of $c_{si}$ are shown in Figure 19. Since the contributions of the 4th and 5th terms are negligible, eq 54 reduces to

$$c_{si} = 0.505 + 0.0018\theta + 4311.5\frac{\sigma}{\theta^2}. \qquad (55)$$

*Specific heat of sea ice between -8.2° and -23°C*

The continuous deposition of $Na_2SO_4 \cdot 10H_2O$ takes place only within this temperature range (Fig. 18). If the rate of deposition with temperature is linear, then the quantity of precipitation at any temperature can be calculated by extrapolating from the initial section of the phase graph. Therefore, in 1 gram of sea ice, there are $w$ grams of water, $w_s$ grams of dissolved salt, $w_p$ grams of precipitated salt with which $\beta w_p$ grams of water are combined in the crystals, where $\beta$ is the mass ratio of $10\,H_2O$ to $Na_2SO_4$ and equals 1.27. Thus, in general, the mass of pure water in the unfrozen solution is

$$w = \frac{\sigma}{s+p} \qquad (56)$$

where $p$ is grams of precipitate (not including its water of crystallization).

The mass of pure ice is

$$m_i = 1 - \sigma - \frac{\sigma}{s+p}(1+\beta p). \quad (57)$$

The change in mass of unfrozen water $w$ as fractional salt content $s$ and associated precipitate $p$ change is

$$dw = -\frac{\sigma(ds+dp)}{(s+p)^2}. \quad (58)$$

(The salinity $\sigma$ is a constant; only the redistribution of salt from liquid to solid or vice versa is of concern.) Figure 18 shows that

$$s+p = \alpha\theta \text{ and } p = \alpha'(\theta+8.2). \quad (59)$$

Substituting $s+p = \alpha\theta$ into eq 58 gives $dw = -(\sigma/\alpha\theta^2)\, d\theta$. Therefore, the heat absorbed by a unit mass of sea ice for a temperature increase $d\theta$ is

$$dq = L_f dw + \left[1 - \sigma - \frac{\sigma}{s+p}(1+\beta p)\right] c_i d\theta + \frac{\sigma}{s+p} c_w d\theta + \left[\frac{\sigma p}{s+p}(1+\beta)\right] c_h d\theta \quad (60)$$

where $c_h$ is the specific heat of the precipitated hydrate.

The expression for specific heat of sea ice is obtained by evaluating $dq/d\theta$ of eq 60, substituting eq 59 in the resulting expression and rearranging, and is expressed as

$$c_{si} = -\frac{\sigma}{\alpha\theta^2} L_f + \frac{\sigma}{\alpha\theta}(c_w - c_i) + (1-\sigma)c_i - \frac{\sigma\alpha'(\theta+8.2)}{\alpha\theta}[\beta c_i - (1+\beta)c_h] \quad (61)$$

by Schwerdtfeger and Pounder (1962). Since $\alpha'/\alpha < 1$, $(\theta+8.2/\theta) < 1$, the terms of $\beta c_i$ and $(1+\beta)c_h$ are of the order of 1, and $\sigma \approx 10^{-3}$, the last term and $\sigma c_i$ can be neglected. Equation 61 reduces to the same form shown in eq 52. Values of $c_{si}$ for salinities ranging from 0 to 0.01 gram of salt per gram of sea ice and temperatures ranging from -2° to -22°C are shown in Figure 19.

**Heat of fusion of sea ice when $0° > \theta > -8.2°C$**

As sea ice has no fixed temperature for phase transition, the heat of fusion $L_{si}$ of sea ice is the amount of heat required to melt 1 gram of sea ice of salinity $\sigma$ and temperature $\theta$. The value of $L_{si}$ is found by integrating eq 4 from $\theta$ to $\theta_m$, where $\theta_m$ is the temperature when the melting is completed and is computed from the relations: $m_i = 1 - \sigma - (\sigma/s)$. When $m_i = 0$ (that is, when melting is complete) and when $s = \alpha\theta_m$ is substituted, $\theta_m$ is $\theta_m = \sigma/\alpha$, after taking into account that $\sigma \ll 1$. If higher order terms of $\sigma$ are neglected,

$$L_{si} = 79.68 - 0.505\theta - 27.3\sigma + 4311.5\frac{\sigma}{\theta} + 0.8\sigma\theta - 0.009\theta^2. \quad (62)$$

The values of $L_{si}$ from eq 62 are shown in Figure 20. For practical purposes, the fifth and sixth terms in the right side of eq 62 can be neglected, and it becomes

$$L_{si} = 79.68 - 0.505\theta - 27.3\sigma + 4311.5\frac{\sigma}{\theta}. \quad (63)$$

**Density and thermal conductivity of sea ice**

The thermal conductivity of sea ice is strongly dependent on composition, that is, the density, salinity and temperature. Schwerdtfeger (1963b) showed that thermal conductivity is mainly determined by salinity at high temperature and by density at low temperatures. As with specific heat, it is simplest to consider ice in the

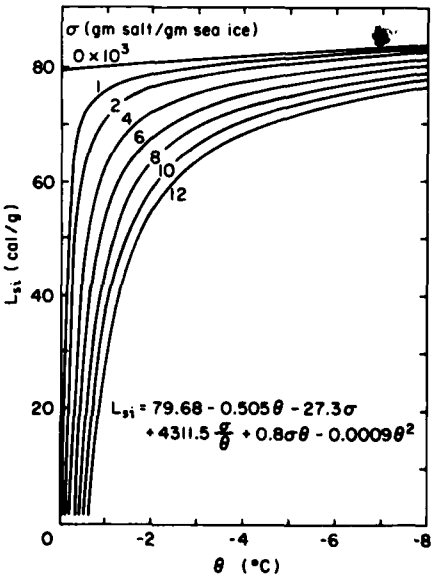


*Figure 20. Latent heat of fusion of sea ice as functions of temperature and salinity. (Modified from Ono 1966.)*

temperature range between 0° and -8.2°C, below which the precipitation of $Na_2SO_4 \cdot 10H_2O$ complicates the analysis.

**Composition and air bubble content of sea ice above -8.2°C**

With $\sigma$ and $s$ defined as before, the mass of unfrozen brine per unit mass of sea ice is $m_b = \sigma/s+\sigma$. The volume of brine is $(\sigma+\sigma/s)/\rho_w(1+s) = \sigma/s\rho_w$, and the volume of ice is $(1-\sigma-\sigma/s)/\rho_i$, where $\rho_w$ and $\rho_i$ are the densities of pure water and ice, respectively. The volumes of brine and ice per unit volume of sea ice are

$$V_b = \rho_{si}\frac{\sigma}{s\rho_w} \tag{64}$$

and

$$V_i = \frac{\rho_{si}}{\rho_i}\left(1-\sigma-\frac{\sigma}{s}\right) \tag{65}$$

where $\rho_{si}$ is the density of sea ice. The volume of air per unit volume of sea ice is

$$V_a = 1-\rho_{si}\left(\frac{\sigma}{s\rho_w}+\frac{1-\sigma-\sigma/s}{\rho_i}\right). \tag{66}$$

If $\rho_w = 0.999$ Mg/m$^3$, $\rho_i = 0.917$ Mg/m$^3$, $s = \alpha\theta$, and $\alpha = -1.82\times10^{-2}$/°C, eq 66 reduces to

$$V_a = 1-\rho_{si}\left(\frac{1-\sigma}{0.917}+\frac{4.98\sigma}{\theta}\right). \tag{67}$$

Figure 21 shows the air bubble content by volume of sea ice as functions of temperature, salinity and density.

Rewriting eq 66, replacing $s = \alpha\theta$, and neglecting the terms containing $\sigma\alpha\theta$ or $\sigma s$ gives the sea ice density as

$$\rho_{si} = \frac{(1-V_a)\rho_w\rho_i\alpha\theta}{\alpha\theta\rho_w-\sigma(\rho_w-\rho_i)}. \tag{68}$$

Since the second term in the denominator is rather small, rewriting and substituting the values of $\rho_w$, $\rho_i$ and $\alpha$ changes eq 68 to

$$\rho_{si} = (1-V_a)\left[1+\frac{\sigma}{\alpha\theta\rho_w}(\rho_w-\rho_i)\right]\rho_i$$

$$= (1-V_a)\left(1-\frac{4.51\sigma}{\theta}\right)0.917. \tag{69}$$

This equation shows that $\rho_{si}$ increases with salinity

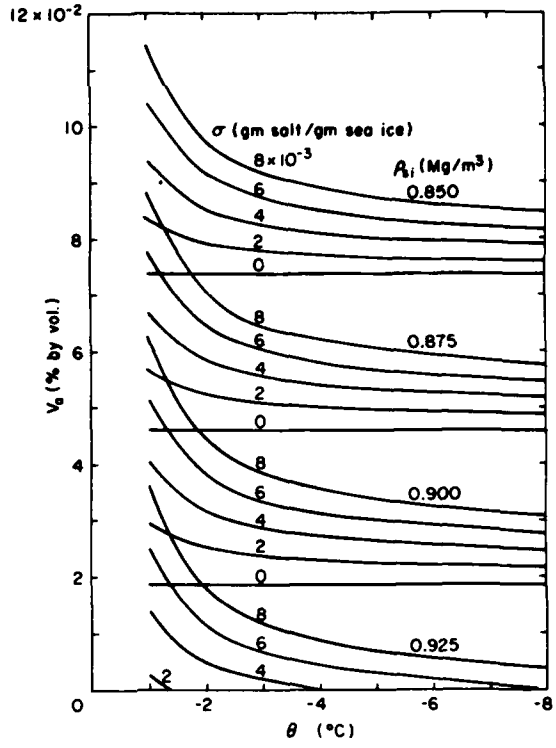


*Figure 21. Fractional air content (by volume) as a function of temperature for sea ice of different salinities and densities.*

if the air content is constant. While the density is temperature-dependent, especially near the freezing point, the dependence diminishes considerably at lower temperatures.

**Thermal conductivity model for sea ice**

Langleben (1960) and others have shown sea ice to consist of pure ice enclosing vertical cylinders of brine that are approximately elliptical in cross section and whose lengths, especially at higher temperatures, are large compared with their average diameters. Anderson (1958), on the other hand, preferred to calculate the thermal conductivity as if the brine pockets were spherical. This assumption may have greater validity at lower temperatures, when the small amount of brine plays a less significant role in determining the thermal conductivity. Based on Maxwell's principle that sea ice consists of uniformly and randomly distributed spherical air bubbles, the thermal conductivity of bubble ice $\lambda_{bi}$ (Schwerdtfeger 1963b) is

$$\lambda_{bi} = \frac{2\lambda_i+\lambda_a-2V_a(\lambda_i-\lambda_a)}{2\lambda_i+\lambda_a+V_a(\lambda_i-\lambda_a)}\lambda_i. \tag{70}$$

For a temperature range of 0° to -20°C, and taking the

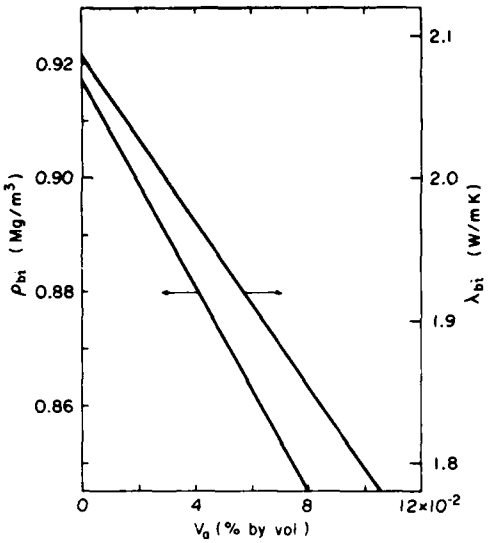


*Figure 22. Density and thermal conductivity of bubbly ice as a function of fractional air content.*

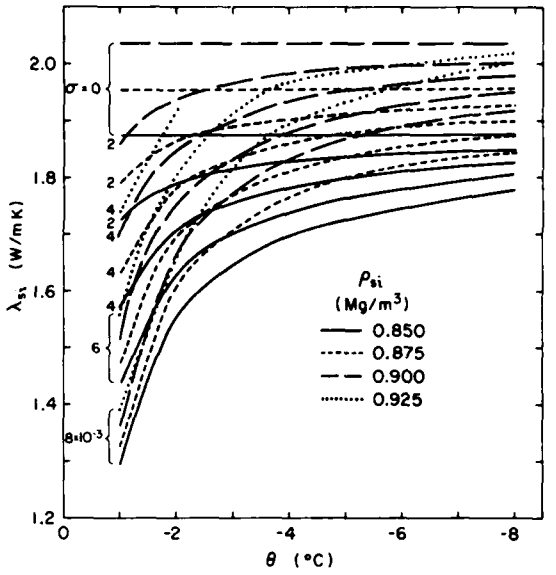


*Figure 23. Effective thermal conductivity of sea ice as a function of temperature for various salinities and densities.*

thermal conductivity of ice $\lambda_i$ to be 2.09 W/m K and the thermal conductivity of air $\lambda_a$ to be $2.51\times10^{-2}$ W/m K, eq 70 is used to calculate $\lambda_{bi}$ and is shown, along with the density of bubbly fresh-water ice, in Figure 22.

If the sea ice consists of parallel configurations of bubbly pure ice and enclosed brine, then the thermal conductivity of sea ice $\lambda_{si}$ is

$$\lambda_{si} = \lambda_{bi} - (\lambda_{bi}-\lambda_b)\frac{\sigma\rho_{si}}{\alpha\rho_w\theta} \qquad (71)$$

where $\lambda_b$ is the thermal conductivity of the brine, which is strongly dependent on the concentration and to a lesser extent on the temperature. If the change in thermal conductivity and fractional salt content is linear at constant temperature for $s < 0.15$, then on the basis of thermal conductivity measurements for NaCl and $Na_2SO_4$ solutions given by Lange and Forker (1952), the value of $\lambda_b$ can be approximated by

$$\lambda_b = 0.4184(1.25+0.030\theta+0.00014\theta^2). \qquad (72)$$

Using $\lambda_b$ from this expression, $\lambda_i$ = 2.09 W/m K. The values of $\lambda_{si}$ calculated from eq 71 are shown in Figure 23.

All the curves (that is, for all densities and salinities) exhibit asymptotic behavior. At lower temperatures, the thermal conductivity of low-salinity sea ice is equal to the value for fresh-water ice.

**Thermal diffusivity of sea ice**

Thermal diffusivity is the most directly observable thermal property, as it is directly related to the rate of temperature change in a medium. It has been seen that the values of $c_{si}$, $\rho_{si}$ and $\lambda_{si}$ are monotonic functions of the temperature; that is, as temperature increases, $c_{si}$ and $\rho_{si}$ also increase but $\lambda_{si}$ decreases. The values of $\alpha_{si} = \lambda_{si}/\rho_{si}c_{si}$ are shown in Figure 24 as functions of temperature and salinity. Note that the values of $\alpha_{si}$ are not greatly affected by density changes as they are for freshwater ice.

**Method of determining thermal diffusivity**

In general, the equation for thermal diffusion is written as

$$c_{si}\rho_{si}\frac{\partial\theta}{\partial t} = \frac{\partial\lambda_{si}}{\partial z}\frac{\partial\theta}{\partial z} + \lambda_{si}\frac{\partial^2\theta}{\partial z^2} \qquad (73)$$

where $t$ is time and $z$ is the depth. Let

$$f = \frac{1}{\lambda_{si}}\frac{\partial\lambda_{si}}{\partial z}\left(\frac{\partial\theta/\partial z}{\partial^2\theta/\partial z^2}\right). \qquad (74)$$

Equation 73 may then be rewritten

$$\frac{\partial\theta}{\partial t} = (1+f)\alpha_{si}\frac{\partial^2\theta}{\partial z^2}. \qquad (75)$$

Letting $\theta_{z,t}$ be the temperature at depth $z$ and time $t$,

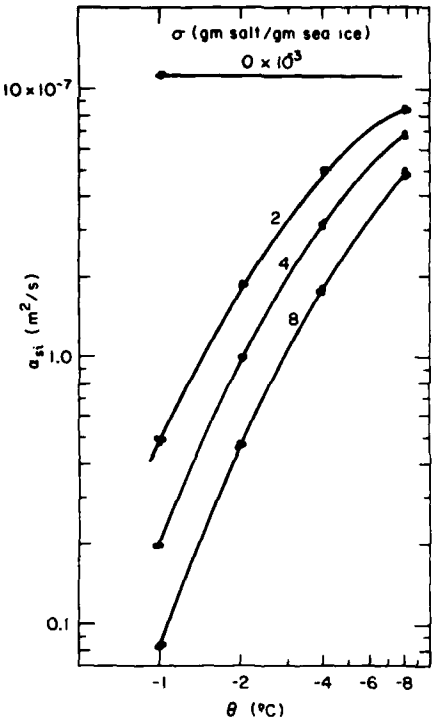


*Figure 24. Thermal diffusivity of sea ice as a function of temperature for various salinities. (The effect of density on $\alpha_{si}$ for a given salinity is insignificant.)*

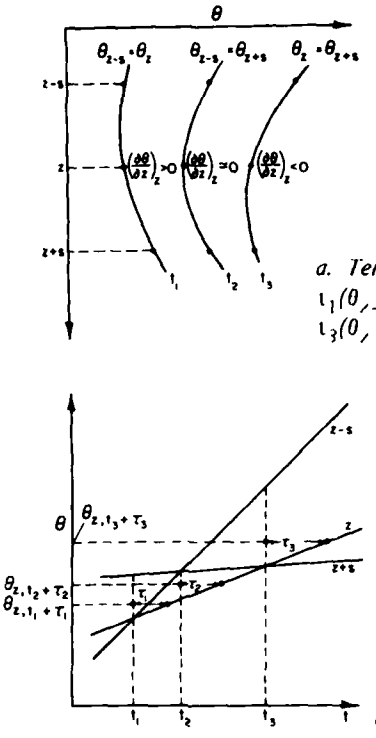


*a. Temperature profile at times $t_1(\theta_{z-s} = \theta_z)$, $t_2(\theta_{z-s} = \theta_{z+s})$ and $t_3(\theta_z = \theta_{z+s})$.*

*b. Graphic determination of times $t_1$, $t_2$ and $t_3$ from actual temperature record.*

*Figure 25. Determining thermal diffusivity from temperature profiles. (At $t_2$, the minimum temperature is close to depth $z$; therefore, it may be assumed that $f = 0$ at approximately $t = t_2$.*

expressing $\theta_{z+s,t}$, $\theta_{z-s,t}$, and $\theta_{z,t+\tau}$ in the Taylor series, and neglecting the higher order terms yields

$$\theta_{z,t+\tau} - \frac{1}{6}(\theta_{z+s,t} + 4\theta_{z,t} + \theta_{z-s,t}) = \tau\frac{\partial\theta}{\partial t} - \frac{s^2}{6}\frac{\partial^2\theta}{\partial z^2}. \quad (76)$$

From eq 75 and 76,

$$\frac{s^2}{6\tau} \equiv [(1+f)\alpha_{si}]_{z,t} \quad (77)$$

and

$$\theta_{z,t+\tau} = \frac{1}{6}(\theta_{z+s,t} + 4\theta_{z,t} + \theta_{z-s,t}). \quad (78)$$

The quantity on the right side of eq 78 can be computed from the experimental data on the temperature changes at depth $z-s$, $z$ and $z+s$, and thus the value of $\theta_{z,t+\tau}$, from which the value of $\tau$ can be determined graphically. Using the values of $s$ and $\tau$, the quantity $s^2/6\tau$ can be computed; it equals $[(1+f)\alpha_{si}]_{z,t}$. If $f = 0$, the value of $\alpha_{si}$ can be determined immediately. By eq 74, $f = 0$ when $\partial\theta/\partial z = 0$, that is, when the temperature is at the minimum or maximum value on the vertical profile. Figure 25a shows temperature profiles at times $t_1(\theta_{z-s} = \theta_z)$, $t_2(\theta_{z-s} = \theta_{z+s})$ and $t_3(\theta_z = \theta_{z+s})$. These times are easily determined from the temperatures as shown in Figure 25b. At each of times $t_1$, $t_2$ and $t_3$, the values of $\frac{1}{6}(\theta_{z-s,t} + 4\theta_{z,t} + \theta_{z+s,t})$ can be computed, and the corresponding values of $\tau_1$, $\tau_2$ and $\tau_3$ can be determined graphically. With the values of $\tau$'s and a given distance increment (which may be varied), the corresponding values of $[(1+f)\alpha_{si}]_{z,t}$ can be obtained using eq 77. However, at time $t_2$ the minimum temperature is closer to depth $z$; therefore, it may be assumed that $f = 0$ at approximately $t_2$, and the value of $[(1+f)\alpha_{si}]_{z,t}$ reduces to $\alpha_{si}$ directly.

## SUMMARY

This report dealt comprehensively with the thermal properties of snow, ice and sea ice. Studies on ice density, thermal expansion and compressibility were

reported. The available data were graphed to make them easier to use and to demonstrate the large discrepancies in the compressibility data. The mechanisms and processes associated with snow density changes due to compaction and destructive, constructive and melt metamorphism were discussed in detail. Equations describing these processes were derived.

Various theories of regelation were reviewed. Data on wire speed as functions of wire material (for example, high and low thermal conductivity or metallic and non-metallic wires), wire radius, driving stress, temperature and contamination were analyzed. Temperature measurements near the moving wire produced some insight into the processes of melting and refreezing. There is still no theory that incorporates all the factors that affect the rate of wire penetration into the ice.

The determination of heat capacity and latent heat of fusion of fresh-water ice was well documented. Slight variations in the reported heat capacity values were noted.

For values of thermal conductivity of ice and snow, however, a much greater scatter was observed. For ice, the large variation was believed to be due to the condition of the sample (such as the level of contamination and the air bubble content). Reproducible data for snow were much more difficult to obtain. Because snow undergoes constant metamorphism as soon as it falls on the ground, its thermal conductivity is evidently not solely a function of its density. However, thermal conductivity of snow was usually reported in terms of density alone without any indication of age or temperature. (The temperature effect is considered to be small.) However, the age of the snow sample and the temperature level under which it had been stored apparently contributed to the dispersion and uncertainty in the data. A brief review and discussion of the effect of air ventilation on effective thermal conductivity and vapor diffusivity were also presented.

Determining the thermal properties of sea ice is considerably more complicated than determining those of fresh-water ice. All the thermal properties, such as specific heat, latent heat and thermal conductivity, are functions of both temperature and salinity (in the temperature range $0°C > \theta > -8.2°C$). In general, the specific heat is much higher than that of the fresh-water ice, especially when the temperature $\theta \to 0°C$. This unusual phenomenon is caused by the fact that when the sea ice temperature rises, melting occurs, adding the latent heat of fusion to the sensible heat. The latent heat of fusion of sea ice is, however, generally lower than that of the fresh-water ice.

In the temperature range $0°C > \theta > -8.2°C$, expressions of the volumetric fraction of air and sea ice density in terms of salinity and temperature were derived. For temperatures lower than -8.2°C the analysis becomes much more complex because of salt precipitation. By considering sea ice to be bubbly pure ice with brine pockets, and by assuming that the components are arranged in parallel (like the connection in resistances), thermal conductivity of sea ice was expressed in terms of bubbly pure ice, brine, salinity, densities of sea ice and water, and temperature. Due to its complex composition and its transient behavior (the migration of brine or the aging effect), sea ice has not been studied extensively; only a handful of field studies have been reported. In the conclusion of this report, an innovative method for determining the thermal diffusivity of sea ice was briefly described.

## LITERATURE CITED


**Abel's, G.** (1893) Daily variation of temperature in snow and the relation between the thermal conductivity of snow and its density. *Meteorol. Vestnik*, vol. 3.

**Anderson, D.L.** (1958) Model for determining sea ice properties. In *Arctic Sea Ice*. Presented at Arctic Sea Ice Conference, Easton, Maryland. Washington, D.C.: U.S. National Academy of Sciences, National Research Council, Publ. 598, p. 148-152.

**Anderson, E.A.** (1976) Point energy and mass balance model of a snow cover. National Oceanic and Atmospheric Administration Technical Report NWS 19.

**Ashworth, T.** (1972) Measurement of the thermal properties of ice. *Proceedings, 4th International Cryogenic Engineering Conference*, p. 377-379.

**Bader, H., R. Haefeli, J. Bucher, J. Neher, O. Eckel and C. Thams** (1939) Snow and its metamorphism. U.S. Army Snow, Ice and Permafrost Research Establishment (SIPRE) Draft Translation 14. AD 030965.

**Barnes, H.T.** (1901) On the density of ice. *Physical Review*, vol. 13, p. 55-59.

**Bass, R., D. Rossberg and G. Zifgler** (1957) The elastic constants of ice. *Zhurnal Physik*, vol. 149, p. 199-203.

**Bottomley, J.T.** (1872) Melting and regelation of ice. *Nature* (London), vol. 5, p. 185.

**Bracht, J.** (1949) On the thermal conductivity of soil and snow, and the heat utilization in soil. *Veröffentl. Geophysikalischen Inst. Univ. Leipzig*, ser. 2, vol. 14, no. 3, p. 147-225.

**Bridgman, P.W.** (1912) Thermodynamic properties of liquid water to 80°C and 1200 kg/cm² pressure. *Proceedings of the American Academy of Arts and Sciences*, vol. 48, p. 309-362.

**Brill, R. and A. Tippe** (1967) Gitterparameter von Eis I bre tiefen Temperaturen. *Acta Crystallographica*, vol. 23, p. 343-345.

**Butkovich, T.R.** (1957) Linear thermal expansion of ice. SIPRE Research Report 40. AD 158192.

**Colbeck, S.C.** (1973) Theory of metamorphism of wet snow. U.S. Army Cold Regions Research and Engineering Laboratory (CRREL) Research Report 313. AD 772692.

**Colbeck, S.C.** (1979) Sintering and compaction of snow containing liquid water. *Philosophical Magazine*, vol. 39, no. 1, p. 13-32.

**Dantl, G.** (1962) Thermal expansion of $H_2O$ and $D_2O$ single crystals. (In German.) *Zhurnal Physik*, vol. 166, no. 1, p. 115-118.

**Dantl, G. (1969)** Elastic moduli of ice. In *Physics of Ice*. p. 223-230.

**Dantl, G. and L. Gregora (1968)** Dicte in hexagonalem eis. *Die Naturwissenschaften*, vol. 55, p. 176.

**Dean, J.W. and K.D. Timmerhaus (963)** Thermal conductivity of solid $H_2O$ and $D_2O$ at low temperature. *Advanced Cryogenic Engineering*, vol. 8, p. 263-267.

**DeQuervain, M.R. (1973)** Snow structure, heat, and mass flux through snow. *Proceedings of Banff Symposia*. International Association of Hydrological Sciences, Publ. No. 97, vol. 1, p. 203-226.

**Devaux, J. (1933)** L'économie radio-thermique des champs de neige et des glaciers. *Annaler Physica*, vol. 20, no. 10, p. 5-67.

**Dickinson, H.C. and N.S. Osborne (1915)** Specific heat and heat of fusion of ice. *Bulletin of the Bureau of Standards (U.S.), Washington*, vol. 12, p. 49-81.

**Dillard, D.S. and K.D. Timmerhaus (1966)** Low temperature thermal conductivity of solidified $H_2O$ and $D_2O$. *Pure Application Cryogenics*, vol. 4, p. 35-44.

**Dorsey, N.E. (1940)** *Properties of Ordinary Water Substance in All Its Phases: Water-Vapor, Water and All the Ices*. New York: Reinhold, 673 p.

**Drake, L.D. and R.L. Shreve (1973)** Pressure melting and regelation of ice by round wires. *Proceedings, Royal Society of London*, vol. A332, p. 51-83.

**Eisenberg, D. and W. Kauzmann (1969)** *Structure and Properties of Water*. London: Oxford University Press, 296 p.

**Fletcher, N.H. (1962)** Surface structure of water and ice. *Philosophical Magazine*, vol. 7, no. 74, p. 255-269.

**Fletcher, N.H. (1968)** Surface structure of water and ice. II. A revised model. *Philosophical Magazine*, vol. 18, p. 1287-1300.

**Flubacher, P., A.J. Leadbetter and J.A. Morrison (1960)** Heat capacity of ice at low temperatures. *Journal of Chemical Physics*, vol. 33, no. 6, p. 1751-1755.

**Frank, F.C. (1967)** Regelation: A supplementary note. *Philosophical Magazine*, vol. 16, p. 1267-1274.

**Giauque, W.F. and J.W. Stout (1936)** The entropy of water and the third law of thermodynamics. The heat capacity of ice from 15 to 273 K. *Journal of American Chemistry Society*, vol. 58, p. 1144-1150.

**Gibbs, J.W. (1877)** On the equilibrium of heterogeneous substances. *Transactions of the Connecticut Academy of Arts and Sciences*, vol. 3, p. 343-524.

**Ginnings, D.C. and R.J. Corruccini (1947)** An improved ice calorimeter—the determination of its calibration factor and the density of ice at 0°C. *Journal of Research of the National Bureau of Standards*, vol. 38, p. 583-591.

**Glen, J.W. (1952)** Experiments on the deformation of ice. *Journal of Glaciology*, vol. 2, p. 111-114.

**Gunn, K.L.S. (1965)** Measurements on new-fallen snow. Stormy Weather Group Scientific Report MW-44, McGill University, Montreal, Canada, 25 p.

**Hahne, E. and U. Grigull (1969)** Some experiments on the regelation of ice. *Physics of Ice, Proceedings of International Symposium*, Munich, p. 320-328.

**Hahne, E. and U. Grigull (1972)** The regelation of ice—A problem of heat conduction. *International Journal of Heat and Mass Transfer*, vol. 15, p. 1057-1066.

**Hobbs, P.V. (1974)** *Ice Physics*. Oxford, England: Clarendon Press.

**Jansson, M. (1901)** The thermal conductivity of snow. *Ofversigt Kgl. Vetenskaps-Akad. Forh.*, vol. 58, p. 207-222.

**Jakob, M. and S. Erk (1928)** Thermal expansion of ice between 0° and -253°. *Z. ges Kälte-Ind*, vol. 35, p. 125-230.

**Jakob, M. and S. Erk (1929)** The thermal conductivity of ice between 0° and -125°C. *Z. ges Kälte-Ind*, vol. 36, p. 229-234.

**Kamb, B. (1961)** The thermodynamic theory of nonhydrostatically stressed solids. *Journal of Geophysical Research*, vol. 66, p. 259-271.

**Kojima, K. (1954)** An experimental study on regelation. *Low Temperature Science*, vol. A13, p. 29-36.

**Kojima, K. (1967)** Densification of seasonal snow layers. *Physics of Snow and Ice, Proceedings of International Conference on Low Temperature Science*, Sapporo, p. 929-952.

**Kondrateva, A.S. (1945)** Thermal conductivity of snow cover and physical processes caused by the temperature gradient. SIPRE Translation 22.

**Landauer, J.K. and H. Plumb (1956)** Measurements on anisotropy of thermal conductivity of ice. SIPRE Research Report 16. AD 094686.

**Lang, N.A. and G.M. Forker (1952)** *Handbook of Chemistry*. Sandusky, Ohio: Handbook Publishers, 8th edition.

**Langleben, M.P. (1960)** Distribution of brine cells in sea ice. *Bulletin of the American Physical Society*, ser. 2, vol. 5, no. 5, p. 359.

**LaPlaca, S.J. and B. Post (1960)** Thermal expansion of ice. *Acta Crystallographica*, vol. 13, no. 6, p. 503-505.

**Leadbetter, A.J. (1965)** The thermodynamic and vibration properties of $H_2O$ ice and $D_2O$ ice. *Proceedings of the Royal Society (London)*, vol. A287, p. 403-425.

**Lee, C.H. (1905)** Effects of temperature and pressure on the thermal conductivities of solids. I. The effects of temperature on the thermal conductivities of some electrical insulators. *Philosophical Transactions of the Royal Society*, vol. A204, p. 433-466.

**Lonsdale, K. (1958)** The structure of ice. *Proceedings of the Royal Society (London)*, vol. A247, p. 424-434.

**Malmgren, F. (1927)** On the properties of sea-ice. In *The Norwegian North Polar Expedition with the "Maud," 1918-1925*, vol. 1.

**Mellor, M. (1964)** Properties of snow. CRREL Cold Regions Science and Engineering Monograph III-A1. AD 611023.

**Moser, H. (1929)** The triple point of water as a fixed point of the temperature scale. (In German.) *Annaler Physika*, vol. 1, no. 55, p. 341-360.

**Nakamura, T. (1966)** A water-like film produced by pressure on the surface of ice crystals. *Physics of Snow and Ice, Proceedings of International Conference on Low Temperature Science*, Sapporo, vol. 1, part 1, p. 247-258.

**Nichols, E.L. (1899)** On the density of ice. *Physical Review*, vol. 8, p. 21-37.

**Nunn, K.R. and D.M. Rowell (1967)** Regelation experiments with wires. *Philosophical Magazine*, vol. 16, p. 1281-1283.

**Nye, J.F. (1967)** Theory of regelation. *Philosophical Magazine*, vol. 16, p. 1249-1266.

**Nye, J.F. (1973)** The motion of ice past obstacles. In *Proceedings of Symposium on the Physics and Chemistry of Ice* (E. Whalley, S.J. Jones and L.W. Gold, Eds.). Ottawa: Royal Society of Canada.

**Ono, N. (1966)** Thermal properties of sea ice. III. On the specific heat of sea ice. *Low Temperature Science*, vol. A24, p. 249-258.

**Pitman, D. and B. Zuckerman (1967)** Effect of thermal conductivity of snow at -99°, -27° and -5°C. *Journal of Applied Physics*, vol. 38, no. 6, p. 2698-2699.

**Pounder, E.R. (1965)** *Physics of Ice*. New York: Pergamon Press.

**Powell, R.W. (1958)** Thermal conductivities and expansion coefficients of water and ice. *Advances in Physics*, vol. 7, p. 276-297.

**Ratcliffe, E.H.** (1962) The thermal conductivity of ice. New data on the temperature coefficient. *Philosophical Magazine*, 8th series, vol. 7, no. 79, p. 1197-1203.

**Richard, T.W. and C.L. Speyers** (1914) The compressibility of ice. *Journal of the American Chemical Society*, vol. 36, p. 491-494.

**Rossini, F.D., D.D. Wagman, W.H. Evens, S. Levine and I. Jaffe** (1952) Selected values of chemical thermodynamic properties. National Bureau of Standards Circular 500, p. 126-128.

**Schwerdtfeger, P. and E.R. Pounder** (1962) Thermal properties of sea ice and energy exchanges between the ice and atmosphere. Defence Research Board Report S-10. Department of National Defence, Ottawa.

**Schwerdtfeger, P.** (1963a) Theoretical derivation of the thermal conductivity and diffusivity of snow. In *The General Assembly of Berkeley*, International Association of Scientific Hydrology Publ. 61, p. 75-81.

**Schwerdtfeger, P.** (1963b) The thermal properties of sea ice. *Journal of Glaciology*, vol. 4, p. 789-807.

**Smith, A.W.** (1925) Latent heat determinations. *Journal of the Optical Society of America*, vol. 10, p. 710-722.

**Sugisaki, M., M. Suga and S. Seki** (1968) Calorimetric study of the glassy state. IV. Heat capacities of glassy water and cubic ice. *Bulletin of the Chemistry Society of Japan*, vol. 41, p. 2591-2599.

**Sulakvelidze, G.K.** (1959) Thermoconductivity equation for porous media containing saturated vapor, water and ice. *Bulletin of the Academy of Sciences, USSR Geophysical Series*, p. 186-188.

**Telford, J.W. and J.S. Turner** (1963) The motion of a wire through ice. *Philosophical Magazine*, vol. 8, p. 527-531.

**Thomson, J.** (1849) Theoretical consideration on the effect of pressure in lowering the freezing point of water. *Translation of the Royal Society of Edinburg, vol. 16, p. 575-580.*

**Thomson, W.** (1850) The effect of pressure in lowering the freezing point of water experimentally demonstrated. *Philosophical Magazine*, vol. 37, p. 1237-1270.

**Townsend, D.W. and R.P. Vickery** (1967) An experiment in regelation. *Philosophical Magazine*, vol. 16, p. 1275-1280.

**Tozuka, S., K. Tusima and G. Wakahama** (1979) Experimental studies on regelation. *Low Temperature Science*, vol. 38, p. 1-14.

**Turpin, G.S. and A.W. Warrington** (1884) On the apparent viscosity of ice. *Philosophical Magazine*, vol. 18, p. 120-123.

**Tyndall, J. and T.H. Huxley** (1857) On the structure and motion of glaciers. *Philosophical Transactions of the Royal Society*, vol. 147, p. 327-346.

**Verhoogen, J.** (1951) The chemical potential of a stressed solid. *Transactions of the American Geophysical Union*, vol. 32, p. 251-258.

**Wakahama, G.** (1968) The metamorphism of wet snow. General Assembly of Bern, International Association of Scientific Hydrology Publ. no. 79, p. 370-379.

**Weertman, J.** (1957) On the sliding of glaciers. *Journal of Glaciology*, vol. 3, p. 33-38.

**Weyl, W.A.** (1951) Surface structure of water and some of its physical and chemical manifestations. *Journal of Colloid Science*, vol. 6, p. 389-405.

**Wolfe, L.H. and J.O. Thieme** (1964) Physical and thermal properties of frozen soil and ice. *Journal of the Society of Petroleum Engineers*, vol. 7, p. 67-72.

**Yen, Y.-C.** (1962) Effective thermal conductivity of ventilated snow. *Journal of Geophysical Research*, vol. 67, no. 3, p. 1091-1098.

**Yen, Y.-C.** (1963) Heat transfer by vapor transfer in ventilated snow. *Journal of Geophysical Research*, vol. 68, no. 4, p. 1093-1101.

**Yen, Y.-C.** (1965) Effective thermal conductivity and water vapor diffusivity of naturally compacted snow. *Journal of Geophysical Research*, vol. 70, p. 1821-1825.

**Yosida, Z.** (1950) Heat transfer by water vapor in a snow cover. *Low Temperature Science*, vol. 5, p. 93-100.

**Yosida, Z.** (1955) Physical studies on deposited snow. I. Thermal properties. Institute of Low Temperature Science Paper 7, Sapporo, p. 19-74.

**Yosida, Z.** (1963) Physical properties of snow. In *Ice and Snow* (W.D. Kingery, Ed.). Cambridge, Mass.: MIT Press, p. 485-527.

**Zarembovitch, A. and A. Kahane** (1964) Détermination des vitesses de propagation d'ondes ultrasonoves longitudinales dans la glace. *C.r. hebd. Seance, Acad. Scie., Paris*, p. 2529-2532.

A facsimile catalog card in Library of Congress MARC format is reproduced below.

Yen, Yin-Chao
Review of thermal properties of snow, ice and sea ice / by Yin-Chao Yen. Hanover, N.H.: U.S. Cold Regions Research and Engineering Laboratory; Springfield, Va.: available from National Technical Information Service, 1981.
v, 35 p., illus.; 28 cm. ( CRREL Report 81-10. )
Bibliography: p. 25.
1. Ice. 2. Sea ice. 3. Snow. 4. Thermal properties. I. United States. Army. Corps of Engineers. II. Army Cold Regions Research and Engineering Laboratory, Hanover, N.H. III. Series: CRREL Report 81-10.


DA
FILM